Morris, J.D., Villinger, H.W., and Klaus, A. (Eds.)
Proceedings of the Ocean Drilling Program, Scientific Results Volume 205

7. CARBON AND NITROGEN GEOCHEMISTRY OF WEDGE SEDIMENTS AT ODP SITE 1040: EVIDENCE FOR SEDIMENT SOURCES, DIAGENETIC HISTORY, AND FLUID MOBILITY[1]

Long Li[2] and Gray E. Bebout[2]

ABSTRACT

We determined the C and N concentrations and isotopic compositions of sediments in the prism sampled during Ocean Drilling Program Legs 170 and 205 offshore Costa Rica, with the goals of evaluating sediment sources and extents of diagenesis and identifying any effects of infiltrating fluids on the sedimentary C and N. The sediments from Leg 170 Site 1040 contain 0.85–1.96 wt% total organic carbon (TOC) with Vienna Peedee belemnite (VPDB) $\delta^{13}C_{VPDB}$ from –26.3‰ to –22.5‰, and 832–2221 ppm total nitrogen (TN) with $\delta^{15}N_{air}$ from +3.5‰ to +6.6‰. Sediment TN concentrations and $\delta^{15}N$ values show dramatic downhole increases within the uppermost 130 m of the section and more gradual downhole decreases from 130 meters below seafloor (mbsf) to the base of the décollement at ~370 mbsf. Concentrations and isotopic compositions of TOC are relatively uniform within the entire section, showing some minor perturbation within the décollement zone. In the uppermost 100 m, upsection increases in TN concentrations at constant TOC concentrations produce significant increases in atomic TOC/TN ratios from ~8 to ~18. Carbonate (calcite) contents in the wedge sediments are generally low (<4 wt%), but the $\delta^{13}C$ and Vienna standard mean ocean water (VSMOW) $\delta^{18}O_{VSMOW}$ values vary significantly from –26.1‰ to +4.1‰ and from +30.0‰ to +35.3‰, respectively. Concentrations and isotopic compositions of TOC and TN

---

[1] Li, L., and Bebout, G.E., 2006. Carbon and nitrogen geochemistry of wedge sediments at ODP Site 1040: evidence for sediment sources, diagenetic history, and fluid mobility. *In* Morris, J.D., Villinger, H.W., and Klaus, A. (Eds.), *Proc. ODP, Sci. Results,* 205, 1–38 [Online]. Available from World Wide Web: <http://www-odp.tamu.edu/publications/205_SR/VOLUME/CHAPTERS/214.PDF>. [Cited YYYY-MM-DD]

[2] Department of Earth and Environmental Sciences, 31 Williams Drive, Lehigh University, Bethlehem PA 18015, USA. Correspondence author: **lol2@lehigh.edu**

Initial receipt: 4 October 2005
Acceptance: 14 June 2006
Web publication: 25 September 2006
Ms 205SR-214

for sediments from Leg 205 Sites 1254 and 1255 overlap well with C-N data for sediments from the same depth intervals obtained during Leg 170 at Site 1040.

At Site 1040, effects of diagenesis on the sedimentary C and N reservoirs appear to be overwhelmed by larger variations in these reservoirs related to changes in paleoproductivity and sediment sources. Previously published ^{10}Be data for the deformed wedge sediments indicate that the sediments are at least 3–4 Ma in age, and as with some major and trace element compositions (e.g., Ba concentrations), the C-N concentration data for the wedge sediments at Site 1040 show more similarity with data for the slope apron section at Site 1041 than with the Pliocene hemipelagic part of the incoming sediment section at Site 1039 (~120–140 mbsf). The deformed wedge sediments below 130 mbsf at Site 1040 are more similar in C-N concentrations to the younger Pleistocene hemipelagic section at Site 1039, but in addition to their differing major and trace element concentrations, they have C and N isotope compositions that indicate a terrestrial organic signature larger than that represented in the hemipelagic sediment section at Site 1039. It is not possible, based on the C-N data presented here, to distinguish between the differing proposed origins of the deformed wedge sediments below ~80 mbsf at Site 1040.

Sediments in the fault zones and décollement show hints of differences in C-N concentrations and isotopic compositions relative to sediments away from these structures, indicating some possible effects of infiltrating fluids on the sedimentary C and N in these zones. However, for C and N concentrations and isotopic compositions, dilution by more locally derived pore waters probably obscured signatures of the passage of more deeply sourced fluids.

INTRODUCTION

Subduction of seafloor sediment and altered oceanic crust carries large volumes of pore water and volatiles structurally bound in minerals into modern convergent margins. Most of the pore water is probably released and expelled back to the surface at shallow depth (<5 km) (Moore and Vrolijk, 1992). In active forearc sedimentary wedges, pore fluid overpressures are created by rapid sediment burial, while thrust faults and décollement provide pathways for fluid mobility (Bolton et al., 1999; Silver et al., 2000; Saffer et al., 2000; Vannucchi and Tobin, 2000). The escape of fluid from depth toward the surface can mobilize not only water-soluble elements but also thermogenic gases (e.g., methane and ammonia) feeding benthic ecosystems (Ruppel and Kinoshita, 2000; Hensen et al., 2004). At greater depths, metamorphic devolatilization can result in metasomatism of the forearc mantle wedge and contribute to arc magmatic volatiles and budgets of volatiles in the deeper mantle (e.g., Bebout, 1995; Mottl et al., 2004). Many questions remain concerning the sources and mobility of fluids in forearc sedimentary wedges, including the extent to which the transport of relatively deeply sourced fluids to shallower parts of prisms can be traced geochemically (see Kastner et al., 1991; Moore and Silver, 2002).

In the Middle America Trench (MAT), fluid dewatered from greater depth and expelled along the décollement and major fault zones (Bolton et al., 1999; Vannucchi and Tobin, 2000; Saito and Goldberg, 2001; Saffer, 2003; Bohrmann et al., 2002) produces pore water anomalies in chlorinity, salinity, cation concentrations, and isotopic ratios (Kimura, Silver, Blum, et al., 1997; Silver et al., 2000; Ruppel and Kinoshita, 2000; Kopf et al., 2000; Morris, Villinger, Klaus, et al., 2003; Saffer and Screaton, 2003). In this paper, we present data for concentrations and isotopic compositions of carbonate, total organic carbon (TOC) and total nitrogen (TN) in the variably deformed sediments from near the toe of the wedge (within 2 km of the trench) of the Central America forearc sampled at Ocean Drilling Program (ODP) Sites 1040, 1254, and 1255 offshore Costa Rica. We consider not only the C-N record of infiltration along structures by fluids mobilized from greater depths but also downhole variations in C-N reservoirs as functions of sediment/organic sources and diagenetic history. Uncertainty remains regarding the sources of the sediments incorporated into the wedge and whether the wedge represents either modern or older sediment offscraping (see discussion by Silver, 2000).

GEOLOGICAL SETTING AND BACKGROUND

The MAT is formed by eastward subduction of the Cocos plate beneath the Caribbean plate (Fig. **F1A**) (Kimura, Silver, Blum, et al., 1997). During ODP Legs 170 and 205, several holes were drilled across the forearc, on the seafloor outboard of the trench, and in the toe of the sediment wedge (within 1.5 km of the trench) off the coast of Costa Rica (Fig. **F1B**). Drilling at Sites 1040 and 1043 recovered sediment from the wedge, including some thrust faults, the décollement, and the subducting seafloor sediment section beneath the décollement, whereas drilling at Sites 1254 and 1255 recovered only wedge sediments from above the décollement (Fig. **F1C**) (Kimura, Silver, Blum, et al., 1997; Morris, Villinger, Klaus, et al., 2003). Based on lithologic and chemical dissimilarities of the wedge sediment at Site 1040 with the sediment in the upper part of the Site 1039 section, including extremely low ^{10}Be concentrations, previous workers have argued that this near-trench part of the wedge represents deformed trench slope sediment or a paleoaccretionary prism rather than sediment presently offscraping from the incoming Cocos plate (see Kimura, Silver, Blum, et al., 1997; Valentine et al., 1997; Silver, 2000; Morris et al., 2002; Morris, Villinger, Klaus, et al., 2003).

F1. Leg 170 and 205 locations, p. 24.

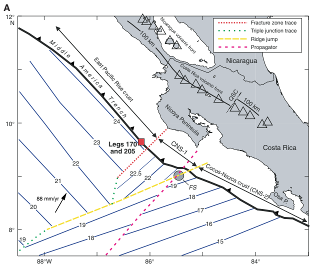

The wedge unit (Unit P1 in Kimura, Silver, Blum, et al., 1997) at Site 1040 consists primarily of relatively homogeneous olive-green to dark olive-green silty clay and can be divided into two subunits (P1A and P1B) according to lithology (Fig. **F1D**) (Kimura, Silver, Blum, et al., 1997). Subunit P1A contains less deformed sediments from 0 to 74.8 meters below seafloor (mbsf), defined by the presence of common matrix-supported sedimentary breccias, composed of angular to subrounded pebble-sized clasts or coarser grained sandy silt and rare silty sand bands. This subunit is thought to largely represent debris flows and turbidites. Rock fragments of andesite, sandstone, and tuff appear in the upper part of this section (Kimura, Silver, Blum, et al., 1997). The more deformed Subunit P1B (74.8–371.2 mbsf), defined by the absence of breccia, is composed of homogeneous silty claystone with few ash layers (Kimura, Silver, Blum, et al., 1997). The subducting sediment section beneath the wedge at Site 1040 repeats the entire incoming sediment section sampled at Site 1039, despite some reduction in sediment thickness at Site 1040 attributed to dewatering (Saffer et al., 2000; McIntosh and Sen, 2000; Saito and Goldberg, 2001; Saffer, 2003). Logging-while-drilling results show high-resolution correlation of Sites

1039 and 1043 (Moritz et al., 2000). ^{10}Be concentrations are very low throughout the wedge section (Unit P1), whereas they display a decay curve from high concentrations just below the décollement to comparatively low concentrations in the lower part of the subducting sediment section, suggesting that little or no sediment is presently being offscraped into the wedge where sampled by Site 1040 (Morris et al., 2002). All of these observations suggest that the Central America margin is presently a nonaccretionary convergent margin, although magnetic fabric observations indicate possible incipient modern underplating of the upper part of the oceanic sedimentary section (Housen and Kanamatsu, 2003).

Fluid venting has been documented along the seafloor at the Costa Rica convergent margin (McAdoo et al., 1996; Kahn et al., 1996; Bohrmann et al., 2002; Hensen et al., 2004). The expelled fluids primarily consist of compaction-related pore water and thermogenic gas hydrate. Fluids are mostly released along active fracture vents, where authigenic carbonates, bacterial mars, solemyid, vesicomyid, mytilid bivalves, and pogonophoran tubeworms are observed (Kahn et al., 1996; Hensen et al., 2004). Mud diapirs provide another pathway for the fluid flow, as imaged by three-dimensional seismic data with the *Alvin* dive program (McAdoo et al., 1996). These fluid processes result in geochemical anomalies in pore fluids in faults and the décollement (e.g., Li, B, Cl, and propane) (Kimura, Silver, Blum, et al., 1997; Chan and Kastner, 2000; Kopf et al., 2000) and surface sediments (e.g., H, C, and O isotopes) (see Hensen et al., 2004).

SAMPLE PREPARATION AND ANALYSIS STRATEGY

The samples used for this study were from several sources, and the sediments have been handled differently depending on the ODP leg on which they were recovered. All of the Leg 205 samples used in this study (Holes 1254A and 1255A) were frozen onboard after removal of pore fluid, producing squeezecakes, whereas most of the Site 1040 samples analyzed in this study were provided by R. Lutz and had been either freeze-dried and stored at room temperature or air-dried at room temperature in plastic bags.

Decomposition of organic matter after drilling, potentially affecting the C-N reservoirs in seafloor sediment samples, could be significant in these samples depending on sediment sample storage methods. The chemical pretreatments (e.g., rinsing with H_2O and dissolutions in HCl) and methods for drying samples must also be carefully considered in efforts to extract information regarding organic and inorganic C-N reservoirs. In order to evaluate these factors, we analyzed frozen Site 1254 and refrigerated Site 1040 sediment samples, which overlap in their depths of recovery with the dried samples obtained from R. Lutz, to compare the results of TOC and nitrogen concentrations and isotope compositions in samples stored (room temperature, refrigerated, and frozen), dried (frozen and low temperatures), and pretreated (H_2O or HCl rinsing) by some commonly employed methods. The results of this testing are provided in the **"Appendix,"** p. 21.

The data presented in this paper were obtained using the following methods. For analyses of carbonate (calcite), samples from Site 1040 were reacted overnight with 100% phosphoric acid at 25°C to extract

CO_2 for measurement of C and O isotope compositions (McCrea, 1950). Concentrations of carbonate were determined by Hg manometry after cryogenic purification of the CO_2 (using a pentane–liquid nitrogen mixture to remove H_2O and SO_2). For analyses of TOC, dried and homogenized sediment was reacted overnight with 1-N HCl and rinsed three times with distilled H_2O before freeze-drying. Decalcified and homogenized samples were loaded into 6-mm (outside diameter) quartz tubes with Cu_xO_x-Cu reagent, sealed at high vacuum, combusted overnight at 910°C, and cracked to release CO_2, which was cryogenically purified using a pentane–liquid nitrogen trap. Concentrations of TOC were obtained by Hg manometry. For analyses of TN, bulk sediment samples without any pretreatment (except two samples from Site 1255; see Table **T1**) were loaded with Cu_xO_x and Cu metal reagents into 9-mm quartz tubes, which were sealed at high vacuum and combusted overnight at 910°C (Sadofsky and Bebout, 2004). The N_2 produced in these combustions was collected for isotope analysis using a molecular sieve at liquid nitrogen temperature after cryogenic purification to remove CO_2, H_2O, and SO_2. Nitrogen concentrations were determined by measuring the *m*/*z* 28 signal for calibrated inlet volumes in the mass spectrometer.

T1. Carbon, nitrogen, and isotopes, p. 34.

All isotope analyses were obtained using a Finnigan MAT 252 mass spectrometer in dual-inlet mode at Lehigh University (Pennsylvania, USA). $\delta^{15}N$, $\delta^{13}C$, and $\delta^{18}O$ values are reported with reference to air, Vienna PeeDee belemnite, and Vienna standard mean ocean water standards, respectively. The reproducibilities of the measured $\delta^{15}N$, $\delta^{13}C$, and $\delta^{18}O$ values were better than 0.2‰ (1σ), and uncertainties for duplicate TOC, N, and carbonate concentration measurements were <5%.

RESULTS

Total N concentrations of sediments from Sites 1040, 1254, and 1255 vary from 832 to 2398 ppm (consistent with the data reported by Kimura, Silver, Blum, et al., 1997, and Morris, Villinger, Klaus, et al., 2003) with $\delta^{15}N$ values from +3.6‰ to +6.6‰ (Table **T1;** Fig. **F2A, F2B**). Both TN concentrations and $\delta^{15}N$ values increase with increasing depth within the uppermost 130 m of the section. Less distinct TN-$\delta^{15}N$ covariance was observed for the deeper part of the section, in which downhole TN and $\delta^{15}N$ decrease slightly with $\delta^{15}N$ values ranging from +3.4‰ to +4.6‰. Total N concentrations and $\delta^{15}N$ values are similar in sediments from Sites 1040 and 1254 obtained from similar depths. Three samples from Site 1255 gave values more scattered than those from Site 1040 (see Table **T1;** Fig. **F2**), possibly because of slightly different pretreatments (H_2O rinsing for two samples and 6-N HCl rinsing for one sample; see the **"Appendix,"** p. 21), but more likely as a result of heterogeneity within the sediments in the wedge (Kimura, Silver, Blum, et al., 1997).

F2. Nitrogen and isotopes, p. 28.

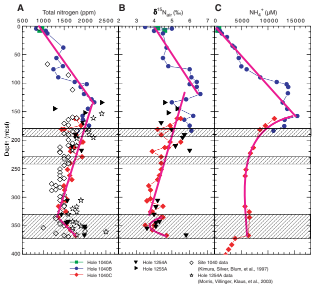

In contrast with the TN concentrations and isotopic data, TOC concentrations and C-isotope compositions show no systematic change with depth (Fig. **F3**). All samples from Sites 1040, 1254, and 1255 contain 0.85–3.06 wt% TOC, with most values between 1 and 2 wt%. These values are near but slightly higher than the concentrations reported by Kimura, Silver, Blum, et al., 1997, and Lutz et al., 2000, with $\delta^{13}C$ values from –26.6‰ to –21.1‰. The only two samples with TOC >2 wt% are from Sites 1254 and 1255. Most sediment samples from Sites 1254 and 1255 have TOC concentrations and $\delta^{13}C$ values similar to those of sedi-

F3. TOC and isotopes, p. 29.

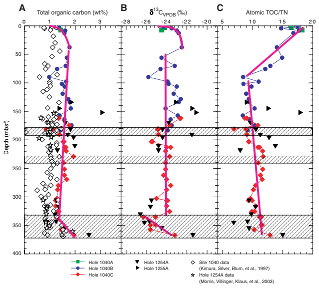

ments obtained from Site 1040 from similar depths (Table **T1;** Fig. **F3A, F3B**).

Carbonate is not abundant in wedge sediments from Site 1040, and all samples examined in this study contain <4 wt% $CaCO_3$ (Table **T1;** Fig. **F4A**). Kimura, Silver, Blum, et al. (1997) reported higher $CaCO_3$ concentrations, as much as 9 wt%, for the same section. These data were obtained using a carbonate carbon analyzer. The reason for these different $CaCO_3$ concentrations is unknown but likely related to the very different analytical methods. In our laboratory, we measure CO_2 yields using a high-vacuum extraction line with a mercury manometer. $\delta^{13}C$ values of carbonates vary significantly from –26.1‰ to +4.1‰, with most values between –8‰ and +4.1‰), and $\delta^{18}O$ values range from +30.0‰ to +36.4‰. As in the case for TOC, $CaCO_3$ concentrations and C- and O-isotope compositions do not show significant coherent change as a function of depth (Fig. **F4**).

F4. Carbonate and isotopes, p. 30.

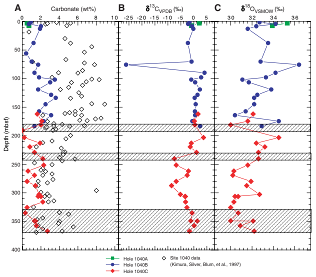

DISCUSSION

Brief Summary of Previous Work on Carbon and Nitrogen Reservoirs in Seafloor Sediments

The C-N variations in the Site 1040 sediment section conceivably resulted from a combination of biogeochemical and sedimentological factors worthy of brief discussion here. Carbon and nitrogen isotope composition of marine sediment can commonly be related to the source (e.g., marine or terrestrial component) of the organic matter. The marine component is characterized by high $\delta^{13}C$ values near –21‰ and $\delta^{15}N$ values of about +8‰ with low C/N of <20, whereas the terrestrial component is characterized by low $\delta^{13}C$ values of about –27‰ and $\delta^{15}N$ values of about +1.8‰ with high C/N from 20 to >200 (Peters et al., 1978; Meyers, 1992; Minoura et al., 1997). However, primary biogenic productivity (Calvert et al., 1992; Minoura et al., 1997; Freudenthal et al., 2001; Ettwein et al., 2001; Pattan et al., 2003; Higginson et al., 2003) or diagenesis (Peters et al., 1978; Sweeney et al., 1978; Rau et al., 1987; Minoura et al., 1997; Sadofsky and Bebout, 2004) are more commonly invoked to produce the variations of C and N concentrations and isotope compositions of marine sediment sections. A variety of processes involving possible isotope fractionation in the water column and sediment section, including N fixation, degradation, nitrification/denitrification, and postburial alteration, have been examined for the effects on C and/or N isotopic compositions. In general, N fixation by phytoplankton at or near the water surface produces little N isotope discrimination; thus, the resultant N compound has $\delta^{15}N$ values close to that of atmosphere (Brandes et al., 1998). However, other processes can produce significant C and N isotope fractionation. The uptake of dissolved inorganic carbon (DIC) and dissolved inorganic nitrogen (DIN) by microbacteria results in organic matter with $\delta^{15}N$ and $\delta^{13}C$ values lower than values for DIC and DIN because of preferential consumption of light C and N isotopes. The magnitude of isotope discrimination depends on the nutrient supply. In a nutrient-rich environment, isotope discrimination results in ^{14}N enrichment in the photosynthetic products, but ^{15}N enrichment in the remaining dissolved nitrate (Voss et al., 1996). If the nutrients are limited, little isotope discrimination occurs, and the $\delta^{15}N$ values of the organic matter should be similar to values for the nitrogenous substrate (Wada and Hattori, 1978; Ostrom et al., 1997). Degradation of particulate organic matter during deposition can increase the C and N isotopic ratio of the remaining organic matter (Thunell and Kepple, 2004).

Postburial diagenetic alteration can also influence the $\delta^{15}N$ values of the sedimentary organic and inorganic N fractions, largely according to redox conditions (Gong and Hollander, 1997; Freudenthal et al., 2001; Lehmann et al., 2002). In the relatively oxidized environment near the sediment/water interface, aerobic organic matter degradation can shift residue organic matter isotopically to slightly heavier values; in anoxic sediments, fixation of ammonium between clay lattices results in a decrease in the $\delta^{15}N$ values of the inorganic and total N (Altabet and Francois, 2001; Freudenthal et al., 2001). The shifts of $\delta^{15}N$ values by these processes are generally regarded as being small (less than ±1‰) (Freudenthal et al., 2001). However, Lehmann et al. (2002) reported much larger $\delta^{15}N$ shifts (3‰) resulting from diagenetic alteration in laboratory incubation experiments. For organic C, some authors have suggested that diagenesis can fractionate C isotopes (Benner et al., 1987; Lehmann et al., 2002), whereas others showed that organic C is isotopically resistant to water-column and/or postburial diagenesis (Meyers and Eadie, 1993; Schelske and Hodell, 1995) and applied $\delta^{13}C$ as a tracer of paleoproductivity and atmospheric pCO_2 levels (Hollander and McKenzie, 1991; Schelske and Hodell, 1991; Fontugne and Calvert, 1992; Brenner et al., 1999).

In summary, the C-N signatures of diagenesis and changes in productivity in seafloor sediments are fairly clear. Diagenesis may in some cases cause a decrease in C/N with decoupled C-N variations of concentrations and isotope compositions (Müller, 1977), whereas productivity changes tend to produce C-N covariance in concentrations and isotope compositions at relatively constant C/N ratios (see discussion by Sadofsky and Bebout, 2004). Without significant superimposed diagenetic effects, linear relationships between C- and N-isotope compositions can in some cases be interpreted as reflecting sources of organic matter (marine vs. terrestrial; e.g., Minoura et al., 1997).

Possible Carbon-Nitrogen Evidence for Diagenetic History at Site 1040

A consideration of the downhole trends in sediment N concentrations and pore water ammonium concentrations indicates that diagenesis did not play a significant role in producing the C-N variations at Site 1040. The sediments show large downhole increases in both N concentrations (from 832 to ~2000 ppm) and $\delta^{15}N$ values (from +3.5‰ to +6.6‰) within the top ~130 mbsf and then gradual downhole decreases in N concentrations (from ~2200 to ~1500 ppm) and $\delta^{15}N$ values (from about +6‰ to about +4‰). Ammonium contents of the interstitial waters are high, reflecting the high sedimentary TN concentrations in the section, and show dramatic downhole increases to ~150 mbsf, then decrease downhole to greater depth. Compared with Site 1039, where sediment C-N concentrations are considerably lower (except in the uppermost part of the section drilled at Site 1039), the concentrations in interstitial water at Site 1040 are as much as 10 times higher for ammonium and 1000 times higher for methane (Kimura, Silver, Blum, et al., 1997). The downhole increases of ammonium concentrations in the pore waters in the upper 180 m indicate increasing diagenetic N release (see Fig. F2). However, the downhole increases of sedimentary TN concentrations in the same interval indicate that any downhole loss of N during diagenesis is overwhelmed by the trend of increase in the sedimentary N reservoir apparently related to other factors.

Downhole variations in the concentrations and isotopic compositions of TOC and carbonate similarly show no obvious signature of diagenesis. Carbonate in the sediments shows no downhole trend in concentration but locally varies significantly in C- and O-isotope compositions (Fig. F4). TOC concentrations remain relatively constant throughout the sediment section (Fig. F3A, F3B), and the downhole increase in N concentrations therefore results in a downhole decrease in TOC/TN ratios, from >18 to <8, within the upper 100 m of the section (Fig. F3C). This variation in TOC/TN resembles a diagenesis signal, as seen in the decrease in TOC/TN downhole at ODP Site 1149 (see Sadofsky and Bebout, 2004; cf. Morris, Villinger, Klaus, et al., 2003); however, the lack of any correlated TOC concentration or isotope shift together with the large downhole increase in TN over this interval argues against diagenesis as the primary effect producing the downhole variation in sediment TOC/TN (Fig. F5).

F5. TOC and TN, p. 31.

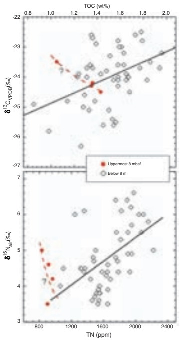

Possible Carbon-Nitrogen Evidence for Sediment Sources in the Wedge Sampled at Site 1040

We suggest that the downhole decline in TOC/TN ratios at Site 1040, including the striking difference between the compositions in the upper ~130 m and those in the wedge section below (i.e., above the décollement), largely reflects variations in the sources of the organic matter deposited in this section. At shallower levels (the less deformed Subunit P1A and the uppermost part of Subunit P1B), the upsection trend of increasing TOC/TN ratios from ~8 at 100 mbsf to >18 at the surface could represent a record of increased terrestrial (continental) organic contribution, largely in sediments interpreted as being debris flow deposits and turbidites and which contain abundant volcanic clasts presumably derived in the volcanic arc. Our N concentration and isotopic data are consistent with this hypothesis, showing upsection decrease from higher TN concentrations and $\delta^{15}N$ values (more marine signature) at ~130 mbsf to lower TN concentrations and $\delta^{15}N$ values (more terrestrial signature) at the top of the section (see Fig. F2). However, the concentrations and isotopic compositions of TOC (Fig. F3A, F3B) in the wedge sediments show no obvious variations over this same interval, perhaps because of a similarity in TOC concentrations and $\delta^{13}C$ values of the terrestrial organic matter (e.g., C3 plant-dominant organic matter characterized by low $\delta^{13}C$ values of approximately –25‰) and marine organic matter. Interestingly, these sediments display homogeneous major and trace element compositions similar to those of the Costa Rica andesites (Kimura, Silver, Blum, et al., 1997). It is unknown whether a significant change in the terrestrial organic component in the sediment could be achieved without producing noticeable change in the overall whole-sediment composition. The increasing terrestrial inputs with time, possibly accompanied by declining marine organic productivity resulting from changes in turbidity, could have resulted in the upsection decreases in N concentrations and $\delta^{15}N$ values with increases in TOC/TN ratios (Fig. F3). This relationship is particularly apparent for the sediments in the upper 50 m containing abundant rock fragments and turbidites but fewer bacterial remnants (Kimura, Silver, Blum, et al., 1997).

In the more deformed wedge below ~130 m (see Fig. **F1**), deformation and the lack of age constraints (see Morris, Villinger, Klaus, et al., 2003) prevent any detailed interpretation of downhole variations in C and N concentrations and isotopic compositions; however, this part of the section likely preserves C-N signatures of sediment sources. Overall, the lower part of the wedge sediment section at Site 1040 displays C-N compositions different from those in the upper ~130 m, showing relatively constant concentrations and isotopic compositions of both TN and TOC, with some more subtle trends (see Figs. **F2, F3**). TOC and TN concentrations, ~1–2 wt% and 1500–2200 ppm, respectively, are similar to those in the upper part of the section drilled at Site 1039 (1.5–2.5 wt% TOC; 1500–2500 ppm TN) (see Fig. **F1**), implying similar overall organic depositional conditions to those at present outboard of the trench at Site 1039 and influenced by the high productivity related to proximity to the shore (see Li and Bebout, 2005). However, the TOC and TN isotopic compositions are different, with the Site 1040 wedge sediments below ~130 mbsf having $\delta^{13}C_{TOC}$ values near –24‰ and $\delta^{15}N$ values near +5‰, and the uppermost part of the Site 1039 section having $\delta^{13}C_{TOC}$ values near –22‰ and $\delta^{15}N$ values near +7‰. This difference could reflect a larger terrestrial organic component in the wedge sediments at Site 1040 (deposited at >3 Ma) relative to the upper part of the Site 1039 section (Pleistocene to the present). On a plot of $\delta^{13}C_{TOC}$ vs. $\delta^{15}N$ (Fig. **F6**), the data for Site 1040 are deflected toward lower $\delta^{13}C_{TOC}$ values from the mixing line between terrestrial and marine components defined by Minoura et al. (1997) (solid mixing line on Fig. **F6**), perhaps a hint of diagenetic shift similar to that at Site 1149 (see field for Site 1149 data on Fig. **F6;** data from Sadofsky and Bebout, 2004). Alternatively, the terrestrial organic material fed into the Site 1040 section had more negative $\delta^{13}C$ values, relative to that deposited more recently at Site 1039, perhaps nearer –28‰ (see the dashed mixing line on Fig. **F6**).

F6. Nitrogen and carbon isotopes, p. 32.

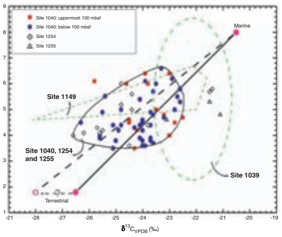

The dissimilarity of the more deformed wedge sediment at Site 1040 below ~80 mbsf and the upper sediment section at Site 1039 does not necessarily preclude formation of the deformed wedge (see Fig. **F7**) by older accretion. Morris et al. (2002) suggested that the uniformly low ^{10}Be concentrations in the Site 1040 wedge sediments could reflect their greater age (older than 3–7 Ma) relative to the sediments in the upper part of the Site 1039 section also sampled at Site 1040 below the décollement. One possibility would be that the more deformed wedge sediments sampled below ~80 mbsf at Site 1040 but above the décollement represent accretion before 3 Ma and that no significant accretion has occurred at this locality since the mid-Pliocene (3 Ma). This accretion would have been approximately contemporaneous with, or somewhat older than, deposition of the lower hemipelagic section at Site 1039, from ~120 to ~140 mbsf. The lower part of the hemipelagic section at Site 1039 is also similar to the more deformed wedge sediments at Site 1040 in its lower content of microfossils (E. Silver, pers. comm., 2005). However, it is problematic to directly compare the deformed wedge section at Site 1040 with the Pliocene section at Site 1039, as Site 1039 must have been located at a greater distance from the trench at ~3 Ma (~260 km using the modern convergence rate of 8.8 cm/yr), and the wedge sediments at Site 1040 could also be somewhat older than the Site 1039 Pliocene hemipelagic section (see Morris et al., 2002; Morris,

F7. Seismic Section CR-20, p. 33.

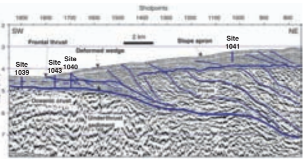

Villinger, Klaus, et al., 2003). Interestingly, organic C and N concentrations in the more deformed wedge sediments at Site 1040 are both higher than in the Pliocene hemipelagic section at Site 1039 (0.5–1.0 wt% TOC; 500–1000 ppm TN; data from Li and Bebout, 2005), perhaps consistent with an increase in organic productivity toward the Pliocene margin. Also, the lower $\delta^{15}N$ values of the more deformed wedge sediments (from +3‰ to +5‰) relative to the $\delta^{15}N$ values in the Pliocene section at Site 1039 (from +5‰ to +7‰) could reflect an increased terrestrial organic component nearer the trench and continent.

A further implication of the Site 1040 deformed wedge representing Pliocene accretion is that this accretion could conceivably have reduced the delivery of the uppermost, more ^{10}Be rich part of the Pliocene sediment section to depths below the Costa Rica arc (because of subduction accretion), perhaps contributing to the modern low-^{10}Be nature of this arc segment (see Valentine et al., 1997; Morris et al., 2002). If this were the case, it would not be necessary to call upon erosion to "dilute" the ^{10}Be signal in the modern Costa Rica arc (see Vannucchi et al., 2003, and discussion in Morris et al., 2002). The absence of a part of the hemipelagic section beneath the modern Costa Rica arc could also produce the proportionally smaller contribution of hemipelagic sediments and larger contribution of carbonate-rich sediment noted for that arc relative to the Nicaragua arc (see Morris, Villinger, Klaus, et al., 2003). However, one important remaining issue related to this consideration of possible paleoaccretion involves the chemical compositions of the sediments (e.g., low Ba concentrations) in the more deformed wedge sediments relative to the presently subducting hemipelagic sediment section as sampled at Site 1039 and below the décollement at Site 1040 (cf. Kimura, Silver, Blum, et al., 1997).

Another, seemingly more likely possibility is that the more deformed wedge sediment section at Site 1040 represents mostly older slope apron sediments also sampled at Site 1041 (8 km upslope from Site 1040), variably deformed within the wedge. The uppermost section of the toe of the wedge is known to move downslope into the trench through creep, slumping, or debris flow (see discussion by Morris, Villinger, Klaus, et al., 2003). This process, if it involved older sediment, could be difficult to distinguish from a scenario of paleoaccretion involving slope sediment, of similar source to that at Site 1041, which was deposited beyond the wedge into the paleotrench then relatively quickly offscraped. The difference between these processes could be somewhat semantic, as it is likely that any sediment deposited onto the extreme toe of the wedge in the Pliocene would also have been deposited somewhat into the trench and onto the top of the sediment section on the incoming plate, where it could then be subducted or offscraped into the deformed wedge. Kimura, Silver, Blum, et al. (1997) reported that the wedge sediments at Site 1040 are more similar in composition to sediments in the slope apron sampled at Site 1041 (e.g., in SiO_2, Fe_2O_3, TiO_2, and Ba concentrations) than to the hemipelagic sediments at Site 1039 (also see data for Site 1043 in Valentine et al., 1997). The uppermost ~80 m of the Site 1040 section consists of less deformed debris flows and turbidites with somewhat different lithology and C-N compositions than the deformed wedge below (Figs. F2, F3), but also similar in major and trace element compositions (SiO_2, Fe_2O_3, TiO_2, and Ba concentrations) to the slope apron sediments recovered at Site 1041 8 km upslope from Site 1040 (see Kimura, Silver, Blum, et al., 1997; Silver, 2000). The chemical compositions and lithologies of these sediments in the upper 80–100 m certainly appear consistent with their being less deformed parts of the slope sediment apron, perhaps ranging in age to more recent than the Pliocene (see the somewhat elevated ^{10}Be in the uppermost part of the Site 1040 wedge section in fig. 4 of Morris et al., 2002).

We did not analyze the C and N concentrations and isotopic compositions of the Site 1041 slope apron sediment section, the upper ~220 m of which is Pliocene to Pleistocene in age (see Kimura, Silver, Blum, et al., 1997). However, TOC and TN concentrations reported by Kimura, Silver, Blum, et al. (1997) (1–1.5 wt% TOC; 1000–2000 ppm TN) for Site 1041 are similar to and only slightly lower than those we report for the deformed wedge sediments at >130 mbsf at Site 1040 (1–2 wt% TOC; 1500–2200 ppm TN) (Figs. F2, F3). The uppermost, less deformed ~100 m of the Site 1040 section has lower N concentrations (decreasing to as low as 1000 ppm) and shows an upsection trend of decreasing δ^{15}N values, relative to values in deeper parts of the wedge section (Fig. F2), that we believe could reflect a less deformed and more intact record of changing organic sources/types.

Possible Sedimentary Carbon and Nitrogen Tracers of Fluid Mobility in Structures

The effect of fluid flow on the C and N concentrations and isotopic compositions of sediments in and near the fault zones and décollement does not appear to be as obvious as the effects on other elements, as recorded by the pore fluid compositions. In the upper fault zone at ~180–193 mbsf at Site 1040, although sedimentary TN, TOC, and carbonate all show hints of decreasing concentrations and isotopic compositions, the magnitudes of the possible shifts are very small (Figs. F2, F3, F4). In the middle fault zone at ~230–240 mbsf, there is no notable difference in the concentrations and isotopic ratios of TN, TOC, and carbonate relative to those of sediments in the adjacent walls. From top to bottom within the décollement zone, sediments show hints of slightly increased TN, TOC, and carbonate concentrations and δ^{15}N, δ^{13}C, and δ^{18}O values, but no changes in carbonate δ^{13}C values (Figs. F2, F3, F4). These changes could be related to fluid flow. Any decreases in TN, TOC, and carbonate concentrations and isotopic compositions in the upper zone could be explained by selective removal of these components during interaction between the sediments and fluids. The décollement zone is divided into a brittle upper part and a ductile lower part, which act as conduit and barrier to fluid flow, respectively (Tobin et al., 2001). However, the variations of concentrations and isotopic compositions of N, TOC, and carbonate are small compared with the effects of productivity and diagenesis unrelated to fluid-sediment interactions, making it difficult to distinguish any possible fluid-related effects from the other heterogeneities, and there are no sharp changes in all these parameters at the boundary between the upper sediment wall and the décollement itself.

The effect of fluid on the sedimentary geochemical C pool is possibly represented in some parts of the Site 1040 section away from fault zones and the décollement. One sediment sample from ~76 mbsf contains carbonate with δ^{13}C of –26.1‰ and δ^{18}O of 36.4‰, which are consistent with biogenic carbonate derived from methane hydrate (von Rad et al., 1996) originating from the decomposition of organic matter at depths of 5–10 km (Hensen et al., 2004; Suess et al., 2001). Authigenic carbonates are in general characterized by extremely low δ^{13}C and high δ^{18}O values, which strongly depend on the environment (Canet et al., 2003; Hensen et al., 2004). As another possible fluid effect, five sediment samples from ~240 to 303 mbsf contain minor carbonate with δ^{13}C values ranging from –5.2‰ to –8.6‰ (Fig. F4B), considerably lower than that of normal marine sedimentary carbonate (0‰ ± 2‰) (Hoefs, 1987) and that of carbonate throughout the rest of the section. These unusually ^{13}C-depleted carbonates could also link to the low-δ^{13}C material (methane and other hydrocarbon compounds) introduced by fluids from greater depths (Kopf et al., 2000).

Nitrogen Flux across the Central America Margin

In our consideration of sedimentary subduction input and arc volcanic output fluxes based on study of C and N in the sediment section at Site 1039, we proposed several uncertainties that complicate efforts at mass balance (Li and Bebout, 2005). One of these is the devolatilization of C and N during very early subduction beneath the wedge. In the fault zones and the décollement, dissolved ammonium in fluids could originate either locally in sediments in the zones or at greater depth, perhaps as deep as 2–10 km (Kopf et al., 2000). Contribution of deeply-sourced ammonium could increase the TN concentrations in the fault zones and produce anomalies in the concentrations and isotopic compositions of TN of sediments or ammonium of interstitial water, as was observed for Cl, Li, B, propane, and some other cations (Silver et al., 2000; Ruppel and Kinoshita, 2000; Morris, Villinger, Klaus, et al., 2003; Kimura, Silver, Blum, et al., 1997; Kopf et al., 2000; Saffer and Screaton, 2003; Müller, 1977). However, obvious concentration or isotopic composition anomalies were not observed in TN of sediment and pore fluid ammonium (Fig. F2). Possible explanations for this lack of an obvious fluid flow signature are that (1) any deeply generated components were diluted through mixing with more locally derived pore water in the fault zones or décollement or diffusive exchange with interstitial water in sediments near fault zones, (2) concentrations of deeply generated ammonium are very low in the fluid infiltrating from greater depth, or (3) concentrations and isotopic compositions of the deeply-sourced fluid did not contrast markedly with those of the more locally derived pore fluids and thus left no signature of their passage.

The lack of an obvious difference in the ammonium concentrations of the fluid in the faults and décollement, relative to those in pore fluids away from these structures, could imply relatively minimal loss of sedimentary N during compaction and deformation at somewhat greater depths experiencing higher temperatures. This hypothesis is consistent with the experimental observation by You and Gieskes (2001) that decomposition of organic matter in the sediment is not important until temperatures exceed 350°C. Sadofsky and Bebout (2003) presented TN concentrations and δ^{15}N values for metamorphosed clastic sedimentary rocks thought to have been subducted to >30 km depths and experienced peak temperatures of <350°C beneath an active accretionary prism and metamorphosed. Sadofsky and Bebout (2003) also demonstrated that the majority of the TN is retained, although largely transferred into clays and low-grade white micas, to these depths without significant change in δ^{15}N values relative to seafloor compositions. However, these authors demonstrated the loss of a relatively high δ^{15}N component of N at very shallow levels (3–5 km, the

Coastal Belt of the Franciscan complex exposed in the California Coast Ranges) and suggested that this loss at <200°C corresponded to removal and mobilization of a more loosely adsorbed component, perhaps nitrate. A study of N concentrations and isotopic compositions in Schistes Lustres and Lago di Cignana metasedimentary rocks (Italian Alps) seemingly documents retention of much of the N inventory in these sediments subducted to depths of as much as 90 km and at temperatures as high as ~625°C (Busigny et al., 2003; see discussion by Sadofsky and Bebout, 2004).

Yet another uncertainty may affect considerations of the broader MAT-to-arc mass balance of N, related to the transit time for the off-trench sediment sections to be subducted beneath the volcanic arc. Turner et al. (2000) suggested that it takes up to several million years for subducted material to be transported from the trench and erupted in arcs. A simple calculation for the MAT indicates that ~2–3 m.y. is required for subducting sediment sections in the MAT to arrive beneath the arc. However, the TOC and TN concentrations of sediments at Site 1039, presently just outboard of the MAT (see Figs. F1, F7), show large increases for the period of 2 Ma to present. One model presented by Li and Bebout (2005) attributes the increase of TOC and TN concentrations (higher productivity) to the greater availability of light and nutrients when the Site 1039 sediment section moved toward the coast with time. A second model suggested by Li and Bebout (2005) attributes the increase of TOC and TN concentrations at Site 1039 to the closure of the Central America Seaway and consequent changes of seawater circulation and climate. If the latter is the case, the sediment section presently beneath the Central America volcanic arc and contributing to arc volcanic gases could contain dramatically different and probably much lower C and N concentrations, given their age of >2–3 Ma. This would cause significant errors in the estimates of sedimentary N inputs into the Central America margin as presented by Li and Bebout (2005). However, most of the more deformed wedge sediments at Site 1040, which appear to be older than 3–4 Ma (Morris et al., 2002), contain very high TOC and TN (1500–2200 ppm N; 1–2 wt% TOC) (Table T1; Figs. F2, F3), nearly as high as concentrations in the uppermost part of the sediment section at Site 1039 (1500–2500 ppm N; 1.5–2.5 wt% TOC) (Li and Bebout, 2005; also note the repetition of the upsection increase in TOC content in the subducting section at Site 1040 beneath the décollement in Lutz et al., 2000). Therefore, it is likely that sediment sections deposited at or near the trench along the older Central America margin (>3 Ma, as represented by the deformed sediment sections sampled at Site 1040) likely experienced similar effects of increased productivity near the continent and trench, and it appears reasonable to use the Site 1039 section as an approximation of the sediment section presently beneath the Central America arc (Li and Bebout, 2005). The Pliocene-aged, lower hemipelagic section at Site 1039 (~120–140 mbsf) contains lower TN and TOC (500–1000 ppm N; 0.5–1.0 wt% TOC), consistent with its having been more distant from the trench, as much as ~260 km (see discussion in Li and Bebout, 2005) at approximately that time.

CONCLUSIONS

Changes in the C-N reservoirs in the sediments sampled at Site 1040 likely reflect changes in productivity and sediment sources with superimposed effects of diagenesis. The deformed wedge sediments at this site, thought to be older than 3 Ma (Morris et al., 2002), have relatively high concentrations of organic matter, containing up to 2400 ppm N and 2 wt% TOC. If these deformed wedge sediments are considered Pliocene or older in age, as indicated by ^{10}Be concentrations (Morris et al., 2002), their C-N concentrations can perhaps be compared with the Pliocene part of the subducting section represented at Site 1039, just outboard of the present-day trench. Differences in the two older sediment reservoirs (Pliocene part of section at Site 1039 and deformed wedge) are consistent with the expected differing proximities of the Site 1039 section and wedge sediments to the trench and continental sediment sources during the Pliocene, with organic productivity and the terrestrial organic component increasing toward the continent. The uppermost, less deformed part of the section drilled at Site 1040 (< 130 m), corresponding to Subunit P1A and the uppermost part of Subunit P1B, shows upsection decreases in TN concentrations (from ~2000 ppm to ~1000 ppm at the top of the section) at a relatively constant TOC concentration of ~1.5 wt%, producing large changes in TOC/TN. We suggest that this increase in TOC/TN (from ~8 at 100 mbsf to >18 at the surface) could represent a somewhat more intact record of changes with time in the sources of the organic matter, with increasing or changing terrestrial/continental organic contributions in these younger, less deformed slope apron sediments interpreted as being debris flow deposits and turbidites. It is not possible, based on our data, to distinguish between origins of the deformed wedge sediments below ~80–100 mbsf as either Pliocene, or somewhat older, near-trench sediment offscraped from the incoming plate or Pliocene or somewhat older, slope sediment deformed within the wedge during slumping and formation of thrust faults resulting from proximity to the evolving décollement. The results presented here also do not bear directly on the issue of whether the Costa Rica convergent margin is at present an erosional margin, on a broader scale (see Vannucchi et al., 2003).

Small perturbations in C-N concentrations and isotopic compositions of deformed sediments in the décollement zone at Site 1040 could reflect enhanced infiltration by C-N-bearing fluids within this structurally complex zone. Although a large fraction of the organic N initially subducted in sediments is thought to be retained to great depths in subduction zones, loss of small amounts of C and N over the extremely large volumes of sediment subducting into this margin could result in C-N mobility sufficient to produce such shifts where fluid flow is highly focused.

ACKNOWLEDGMENTS

This research used samples and/or data provided by the Ocean Drilling Program (ODP). ODP is funded by the U.S. National Science Foundation (NSF) and participating countries under management of Joint Oceanographic Institutions (JOI), Inc. This study was partly funded by JOI United States Science Support Program (JOI-USSSP). We thank Leg 205 Co-Chief Scientists J.D. Morris and H. Villinger, ODP Staff Scientist Adam Klaus, and the Scientific Party of Leg 205 for their support of our shore-based research. We also thank R. Lutz for providing most of the Site 1040 samples and J. Firth for his help in procuring Leg 205 sediments from the ODP Gulf Coast Core Repository (College Station, Texas). We acknowledge extremely useful communications with Dave Scholl, Don Fisher, Eli Silver, and Kirk McIntosh that helped us shape the interpretations sections of this manuscript. Any errors in these sections are, of course, solely our responsibility. Finally, we thank Peter Clift and Jeff Ryan for their constructive reviews and Julie Morris for her editorial handling of this manuscript.

REFERENCES

Altabet, M.A., and Francois, R., 2001. Nitrogen isotope biogeochemistry of the Antarctic polar frontal zone at 170°W. *Deep-Sea Res., Part II,* 48(19–20):4247–4273. **doi:10.1016/S0967-0645(01)00088-1**

Bebout, G.E., 1995. The impact of subduction-zone metamorphism on mantle-ocean chemical cycling. *Chem. Geol.,* 126(2):191–218. **doi:10.1016/0009-2541(95)00118-5**

Bebout, G.E., and Fogel, M.L., 1992. Nitrogen-isotope compositions of metasedimentary rocks in the Catalina schist, California: implications for metamorphic devolatilization history. *Geochim. Cosmochim. Acta,* 56(7):239–249. **doi:10.1016/0016-7037(92)90363-N**

Bebout, G.E., and Sadofsky, S.J., 2004. $\delta^{15}N$ analyses of ammonium-rich silicate minerals by sealed-tube extractions and dual inlet, viscous-flow mass spectrometry. *In* de Groot, P.A. (Ed.), *Handbook of Stable Isotope Techniques:* Amsterdam (Elsevier).

Benner, R., Fogel, M.L., Sprague, E.K., and Hodson, R.E., 1987. Depletion of ^{13}C in lignin and its implications for stable carbon isotope studies. *Nature (London, U. K.),* 329(6141):708–710. **doi:10.1038/329708a0**

Bohrmann, G., Heeschen, K., Jung, C., Weinrebe, W., Baranov, B., Cailleau, B., Heath, R., Hühnerbach, V., Hort, M., Masson, D., and Trummer, I., 2002. Widespread fluid expulsion along the seafloor of the Costa Rica convergent margin. *Terra Nova,* 14(2):69–79. **doi:10.1046/j.1365-3121.2002.00400.x**

Bolton, A.J., Clennell, M.B., and Maltman, A.J., 1999. Nonlinear stress dependence of permeability: a mechanism for episodic fluid flow in accretionary wedges. *Geology,* 27(3):239–242. **doi:10.1130/0091-7613(1999)027<0239:NSDOPA>2.3.CO;2**

Brandes, J.A., Devol, A.H., Yashinari, T., Jayakumar, D.A., and Naqvi, S.W.A., 1998. Isotopic composition of nitrate in the central Arabian Sea and tropical North Pacific: a tracer for mixing and nitrogen cycles. *Limnol. Oceanogr.,* 43(7):1680–1689.

Brenner, M., Whitmore, T.J., Curtis, J.H., Hodell, D.A., and Schelske, C.L., 1999. Stable isotope ($\delta^{13}C$ and $\delta^{15}N$) signatures of sedimented organic matter as indicators of historic lake trophic state. *J. Paleolimnol.,* 22(2):205–221. **doi:10.1023/A:1008078222806**

Busigny, V., Cartigny, P., Philippot, P., Ader, M., and Javoy, M., 2003. Massive recycling of nitrogen and other fluid-mobile elements (K, Rb, Cs, H) in a cold slab environment: evidence from HP to UHP oceanic metasediments of the Schistes Lustrés nappe (western Alps, Europe). *Earth Planet. Sci. Lett.,* 215(1–2):27–42. **doi:10.1016/S0012-821X(03)00453-9**

Calvert, S.E., Nielsen, B., and Fontugne, M.R., 1992. Evidence from nitrogen isotope ratios for enhanced productivity during formation of eastern Mediterranean sapropels. *Nature (London, U. K.),* 359:223–225. **doi:10.1038/359223a0**

Canet, C., Prol-Ledesma, R.M., Melgarejo, J.-C., and Reyes, A., 2003. Methane-related carbonates formed at submarine hydrothermal springs: a new setting for microbially-derived carbonates? *Mar. Geol.,* 199(3–4):245–261. **doi:10.1016/S0025-3227(03)00193-2**

Chan, L.-H., and Kastner, M., 2000. Lithium isotopic compositions of pore fluids and sediments in the Costa Rica subduction zone: implications for fluid processes and sediment contribution to the arc volcanoes. *Earth Planet. Sci. Lett.,* 183(1–2):275–290. **doi:10.1016/S0012-821X(00)00275-2**

Ettwein, V.J., Stickley, C.E., Maslin, M.A., Laurie, E.R., Rosell-Melé, A., Vidal, L., and Brownless, M., 2001. Fluctuations in productivity and upwelling intensity at Site 1083 during the intensification of the Northern Hemisphere glaciation (2.40–2.65 Ma). *In* Wefer, G., Berger, W.H., and Richter, C. (Eds.), *Proc. ODP, Sci. Results,* 175 [Online]. Available from World Wide Web: <**http://www-odp.tamu.edu/publications/175_SR/chap_18/chap_18.htm**>. [Cited 2005-10-01]

Fontugne, M.R., and Calvert, S.E., 1992. Late Pleistocene variability of the carbon isotopic composition of organic matter in the eastern Mediterranean: monitor of changes in carbon sources and atmospheric CO_2 levels. *Paleoceanography,* 7:1–20.

Freudenthal, T., Neuer, S., Meggers, H., Davenport, R., and Wefer, G., 2001. Influence of lateral particle advection and organic matter degradation on sediment accumulation and stable nitrogen isotope ratios along a productivity gradient in the Canary Islands region. *Mar. Geol.,* 177(1–2):93–109. **doi:10.1016/S0025-3227(01)00126-8**

Gong, C., and Hollander, D.J., 1997. Differential contribution of bacteria to sedimentary organic matter in oxic and anoxic environments, Santa Monica Basin, California. *Org. Geochem.,* 26(9–10):545–563. **doi:10.1016/S0146-6380(97)00018-1**

Hensen, C., Wallman, K., Schmidt, M., Ranero, C.R., and Suess, E., 2004. Fluid expulsion related to mud extrusion off Costa Rica—a window to the subducting slab. *Geology,* 32(3):201–204. **doi:10.1130/G20119.1**

Higginson, M.J., Maxwell, J.R., and Altabet, M.A., 2003. Nitrogen isotope and chlorine paleoproductivity records from the northern South China Sea: remote vs. local forcing of millennial- and orbital-scale variability. *In* Clemens, S.C., Wang, P., and Prell, W.L. (Eds.), *Asian Monsoons and Global Linkages on Milankovitch and Sub-Milankovitch Time Scales*. Mar. Geol., 201:223–250.

Hoefs, J., 1987. *Stable Isotope Geochemistry* (3rd ed.): Berlin (Springer).

Hollander, D.J., and McKenzie, J.A., 1991. CO_2 control on carbon-isotope fractionation during aqueous photosynthesis: a paleo–pCO_2 barometer. *Geology,* 19(9):929–932. **doi:10.1130/0091-7613(1991)019<0929:CCOCIF>2.3.CO;2**

Housen, B.A., and Kanamatsu, T., 2003. Magnetic fabrics from the Costa Rica margin: sediment deformation during the initial dewatering and underplating process. *Earth Planet. Sci. Lett.,* 206(1–2):215–228. **doi:10.1016/S0012-821X(02)01076-2**

Kahn, L.M., Silver, E.A., Orange, D., Kochevar, R., and McAdoo, B., 1996. Surficial evidence of fluid expulsion from the Costa Rica accretionary prism. *Geophys. Res. Lett.,* 23(8):887–890. **doi:10.1029/96GL00732**

Kastner, M., Elderfield, H., and Martin, J.B., 1991. Fluids in convergent margins: what do we know about their composition, origin, role in diagenesis and importance for oceanic chemical fluxes? *Philos. Trans. R. Soc. London, Ser. A,* 335:243–259.

Kimura, G., Silver, E.A., Blum, P., et al., 1997. *Proc. ODP, Init. Repts.,* 170: College Station, TX (Ocean Drilling Program). [**HTML**]

Kopf, A., Deyhle, A., and Zuleger, E., 2000. Evidence for deep fluid circulation and gas hydrate dissociation using boron and boron isotopes of pore fluids in forearc sediments from Costa Rica (ODP Leg 170). *Mar. Geol.,* 167(1–2):1–28. **doi:10.1016/S0025-3227(00)00026-8**

Krishnamurthy, R.V., Syrup, K., and Long, A., 1999. Is selective preservation of nitrogenous organic matter reflected in the $\delta^{13}C$ signal of lacustrine sediments? *Chem. Geol.,* 158(3–4):165–172. **doi:10.1016/S0009-2541(99)00020-0**

Lehmann, M.F., Bernasconi, S.M., Barbieri, A., and McKenzie, J.A., 2002. Preservation of organic matter and alteration of its carbon and nitrogen isotope composition during simulated and in situ early sedimentary diagenesis. *Geochim. Cosmochim. Acta,* 66(20):3573–3584. **doi:10.1016/S0016-7037(02)00968-7**

Li, L., and Bebout, G.E., 2005. Carbon and nitrogen geochemistry of sediments in the Central American convergent margin: insights regarding subduction input fluxes, diagenesis, and paleoproductivity. *J. Geophys. Res.,* 110:B11202. **doi:10.1029/2004JB003276**

Lutz, R., Gieren, B., Lückge, A., Wilkes, H., and Littke, R., 2000. Composition of organic matter in subducted and unsubducted sediments off the Nicoya Peninsula, Costa Rica (ODP Leg 170, Sites 1039 and 1040). *Org. Geochem.,* 31(12):1597–1610. **doi:10.1016/S0146-6380(00)00089-9**

McAdoo, B.G., Orange, D.L., Silver, E.A., McIntosh, K., Abott, L., Galewsky, J., Kahn, L., and Protti, M., 1996. Seafloor structural observations, Costa Rica accretionary prism. *Geophys. Res. Lett.,* 23(8):883–886. **doi:10.1029/96GL00731**

McCrea, J.M., 1950. On the isotopic chemistry of carbonates and a paleotemperature scale. *J. Chem. Phys.,* 18(6):849–857. **doi:10.1063/1.1747785**

McIntosh, K.D., and Sen, M.K., 2000. Geophysical evidence for dewatering and deformation processes in the ODP Leg 170 area offshore Costa Rica. *Earth Planet. Sci. Lett.,* 178(1–2):125–138. **doi:10.1016/S0012-821X(00)00069-8**

Meyers, P.A., 1992. Organic matter variations in sediments from DSDP Sites 362 and 532: evidence of upwelling changes in the Benguela Current upwelling system. *In* Summerhayes, C.P., Prell, W.L., and Emeis, K.C. (Eds.), *Upwelling Systems: Evolution Since the Early Miocene.* Spec. Publ.—Geol. Soc. London, 64:323–329.

Meyers, P.A., and Eadie, B.J., 1993. Sources, degradation and recycling of organic matter associated with sinking particles in Lake Michigan. *Org. Geochem.,* 20(1):47–56. **doi:10.1016/0146-6380(93)90080-U**

Minoura, K., Hoshino, K., Nakamura, T., and Wada, E., 1997. Late Pleistoncene–Holocene paleoproductivity circulation in the Japan Sea: sea-level control on $\delta^{13}C$ and $\delta^{15}N$ records of sediment organic material. *Palaeogeogr., Palaeoclimatol., Palaeoecol.,* 135(1–4):41–50. **doi:10.1016/S0031-0182(97)00026-6**

Moore, G.F., and Silver, E., 2002. Fluid flow in accreting and eroding convergent margins. *JOIDES J.,* 28:91–96.

Moore, J.C., and Vrolijk, P., 1992. Fluids in accretionary prisms. *Rev. Geophys.,* 30:113–135.

Moritz, E., Bornholdt, S., Westphal, H., and Meschede, M., 2000. Neural network interpretation of LWD data (ODP Leg 170) confirms complete sediment subduction at the Costa Rica convergent margin. *Earth Planet. Sci. Lett.,* 174(3–4):301–312. **doi:10.1016/S0012-821X(99)00270-8**

Morris, J., Valentine, R., and Harrison, T., 2002. ^{10}Be imaging of sediment accretion, subduction along the northeast Japan and Costa Rica convergent margins. *Geology,* 30(1):59–62. **doi:10.1130/0091-7613(2002)030<0059:BIOSAA>2.0.CO;2**

Morris, J.D., Villinger, H.W., Klaus, A., et al., 2003. *Proc. ODP, Init. Repts.,* 205 [CD-ROM]. Available from: Ocean Drilling Program, Texas A&M University, College Station TX 77845-9547, USA. [**HTML**]

Mottl, M.J., Wheat, C.G., Fryer, P., Gharib, J., and Martin, J.B., 2004. Chemistry of springs across the Mariana forearc shows progressive devolatilization of the subducting plate. *Geochim. Cosmochim. Acta,* 68(23):4915–4933. **doi:10.1016/j.gca.2004.05.037**

Müller, P.J., 1977. C/N ratios in Pacific deep sea sediments: effect of inorganic ammonium and organic nitrogen compounds sorbed by clays. *Geochim. Cosmochim. Acta,* 41(6):765–776. **doi:10.1016/0016-7037(77)90047-3**

Ostrom, N.E., Macko, S.A., Deible, D., and Thompson, R.J., 1997. Seasonal variation in the stable carbon and nitrogen isotope biogeochemistry of a coastal cold ocean environment. *Geochim. Cosmochim. Acta,* 61(14):2929–2942. **doi:10.1016/S0016-7037(97)00131-2**

Pattan, J.N., Masuzawa, T., Naidu, P.D., Parthiban, G., and Yamamoto, M., 2003. Productivity fluctuations in the southeastern Arabian Sea during the last 140 ka. *Palaeogeogr., Palaeoclimatol., Palaeoecol.,* 193(3–4):575–590. **doi:10.1016/S0031-0182(03)00267-0**

Peters, K.E., Sweeney, R.E., and Kaplan, I.R., 1978. Correlation of carbon and nitrogen stable isotope ratios in sedimentary organic matter. *Limnol. Oceanogr.,* 23:598–604.

Rau, G.H., Arthur, M.A., and Dean, W.E., 1987. $^{15}N/^{14}N$ variations in Cretaceous Atlantic sedimentary sequences: implication for past changes in marine nitrogen biogeochemistry. *Earth Planet. Sci. Lett.,* 82(3–4):269–279. **doi:10.1016/0012-821X(87)90201-9**

Ruppel, C., and Kinoshita, M., 2000. Fluid, methane, and energy flux in an active margin gas hydrate province, offshore Costa Rica. *Earth Planet. Sci. Lett.,* 179(1):153–165. **doi:10.1016/S0012-821X(00)00096-0**

Sadofsky, S.J., and Bebout, G.E., 2000. Ammonium partitioning and nitrogen-isotope fractionation among coexisting micas during high-temperature fluid-rock interactions: examples from the New England Appalachians. *Geochim. Cosmochim. Acta,* 64(16):2835–2849. **doi:10.1016/S0016-7037(00)00393-8**

Sadofsky, S.J., and Bebout, G.E., 2003. Record of forearc devolatilization in low-T, high-P/T metasedimentary suites: significance for models of convergent margin chemical cycling. *Geochem., Geophys., Geosyst.,* 4(4):9003. **doi:10.1029/2002GC000412**

Sadofsky, S.J., and Bebout, G.E., 2004. Nitrogen geochemistry of subducting sediments: new results from the Izu-Bonin-Mariana margin and insights regarding global nitrogen subduction. *Geochem., Geophys., Geosyst.,* 5(3):Q03I15. **doi:10.1029/2003GC000543**

Saffer, D.M., 2003. Pore pressure development and progressive dewatering in underthrust sediments at the Costa Rican subduction margin: comparison with northern Barbados and Nankai. *J. Geophys. Res.,* 108(B5):2261–2276. **doi:10.1029/2002JB001787**

Saffer, D.M., and Screaton, E.J., 2003. Fluid flow at the toe of convergent margins: interpretation of sharp pore-water geochemical gradients. *Earth Planet. Sci. Lett.,* 213(3–4):261–270. **doi:10.1016/S0012-821X(03)00343-1**

Saffer, D.M., Silver, E.A., Fisher, A.T., Tobin, H., and Moran, K., 2000. Inferred pore pressures at the Costa Rica subduction zone: implications for dewatering processes. *Earth Planet. Sci. Lett.,* 177(3–4):193–207. **doi:10.1016/S0012-821X(00)00048-0**

Saito, S., and Goldberg, D., 2001. Compaction and dewatering processes of the oceanic sediments in the Costa Rica and Barbados subduction zones: estimates from in situ physical property measurements. *Earth Planet. Sci. Lett.,* 191(3–4):283–293. **doi:10.1016/S0012-821X(01)00403-4**

Schelske, C.L., and Hodell, D.A., 1991. Recent changes in productivity and climate of Lake Ontario detected by isotopic analysis of sediments. *Limnol. Oceanogr.,* 36:961–975.

Schelske, C.L., and Hodell, D.A., 1995. Using carbon isotopes of bulk sedimentary organic matter to reconstruct the history of nutrient loading and eutrophication in Lake Erie. *Limnol. Oceanogr.,* 40:918–929.

Silver, E.A., 2000. Leg 170: synthesis of fluid-structural relationships of the Pacific margin of Costa Rica. *In* Silver, E.A., Kimura, G., Blum, P., and Shipley, T.H. (Eds.), *Proc. ODP, Sci. Results,* 170 [Online]. Available from World Wide Web: <**http://www-odp.tamu.edu/publications/170_SR/chap_04/chap_04.htm**>. [Cited 2005-10-01]

Silver, E., Fisher, A., Saffer, D., Kastner, M., Morris, J., and McIntosh, K., 2000. Fluid flow paths in the Middle America Trench and Costa Rica margin. *Geology,* 28(8):679–682. **doi:10.1130/0091-7613(2000)028<0679:FFPITM>2.3.CO;2**

Suess, E., Torres, M.E., Bohrmann, G., Collier, R.W., Rickert, D., Goldfinger, C., Linke, P., Heuser, A., Sahling, H., Heeschen, K., Jung, C., Nakamura, K., Greinert, J., Pfannkuche, O., Tréhu, A., Klinkhammer, G., Whiticar, M.J., Eisenhauer, A., Teichert, B., and Elvert, M., 2001. Sea floor methane hydrates at Hydrate Ridge, Cascadia margin. *In* Paull, C.K., and Dillon, W.P. (Eds.), *Natural Gas Hydrates: Occurrence, Distribution, and Detection.* Geophys. Monogr., 124:87–98.

Sweeney, R.E., Liu, K.K., and Kaplan, I.R., 1978. Oceanic nitrogen isotopes and their uses in determining the source of sedimentary nitrogen. *In* Robinson, B.W. (Ed.), *Stable Isotopes in the Earth Sciences.* DSIR Bull. (N. Z.), 220:9–26.

Thunell, R.C., and Kepple, A.B., 2004. Glacial–Holocene δ^{15}N record from the Gulf of Tehuantepec, Mexico: implications for denitrification in the eastern equatorial Pacific and changes in atmospheric N_2O. *Global Biogeochem. Cycles,* 18:GB1001. **doi:10.1029/2002GB002028**

Tobin, H., Vannuchi, P., and Meschede, M., 2001. Structure, inferred mechanical properties, and implications for fluid transport in the décollement zone, Costa Rica convergent margin. *Geology,* 29(10):907–910. **doi:10.1130/0091-7613(2001)029<0907:SIMPAI>2.0.CO;2**

Tolun, L., Çagatay, M.N., and Carrigan, W.J., 2002. Organic geochemistry and origin of late Glacial–Holocene sapropelic layers and associated sediments in Marmara Sea. *Mar. Geol.,* 190(1–2):47–60. **doi:10.1016/S0025-3227(02)00342-0**

Turner, S.P., George, R.M.M., Evans, P.J., Hawkesworth, C.J., and Zellmer, G.F., 2000. Time-scales of magma formation, ascent and storage beneath subduction-zone volcanoes. *Philos. Trans. R. Soc. London, Ser. A,* 358:1443–1464.

Valentine, R., Morris, J.D., and Duncan, D., 1997. Sediment subduction, accretion, underplating and arc volcanism along the margin of Costa Rica: constraints from Ba, Zn, Ni, and ^{10}Be concentrations. *Eos, Trans. Am. Geophys. Union,* 78:F673.

Vannucchi, P., Ranero, C.R., Galeotti, S., Straub, S.M., Scholl, D.W., and McDougall-Ried, K., 2003. Fast rates of subduction erosion along the Costa Rica Pacific margin: implications for nonsteady rates of crustal recycling at subduction zones. *J. Geophys. Res.,* 108(B11):2511. **doi:10.1029/2002JB002207**

Vannucchi, P., and Tobin, H., 2000. Deformation structures and implications for fluid flow at the Costa Rica convergent margin, ODP Sites 1040 and 1043, Leg 170. *J. Struct. Geol.,* 22(8):1087–1103. **doi:10.1016/S0191-8141(00)00027-4**

von Rad, U., Rösch, H., Berner, U., Geyh, M., Marchig, V., and Schulz, H., 1996. Authigenic carbonates derived from oxidized methane vented from the Makran accretionary prism off Pakistan. *Mar. Geol.,* 136(1–2):55–77. **doi:10.1016/S0025-3227(96)00017-5**

Voss, M., Altabet, M.A., and von Bodungen, B., 1996. δ^{15}N in sedimenting particles as indicator of euphotic-zone processes. *Deep-Sea Res., Part I,* 43(1):33–47. **doi:10.1016/0967-0637(95)00099-2**

Wada, E., and Hattori, A., 1978. Nitrogen isotope effects in the assimilation of inorganic nitrogeneous compounds by marine diatoms. *Geomicrobiol. J.,* 1:85–01.

You, C.-F., and Gieskes, J.M., 2001. Hydrothermal alteration of hemi-pelagic sediments: experimental evaluation of geochemical processes in shallow subduction zones. *Appl. Geochem.,* 16(9–10):1055–1066. **doi:10.1016/S0883-2927(01)00024-5**

APPENDIX

Evaluation of the Effects of Varying Storage and Pretreatment on Seafloor Sediment Carbon-Nitrogen Concentrations and Isotope Compositions

Prior to conducting our analytical work on the Site 1040 samples, we undertook a series of tests to (1) investigate the possible effects (e.g., decomposition) of long-term storage of seafloor sediments under refrigeration and therefore investigate our ability to exploit the extensive archives of sediment sections obtained from oceans and lakes with confidence that the organic C-N reservoirs have been preserved, (2) examine whether low-temperature heating during drying causes decomposition of organic matter affecting the C-N compositions, and (3) identify any possible effects of H_2O rinsing and treatments with HCl on the organic and inorganic N reservoirs.

Method Description

For determinations of TOC concentration and isotopic composition, each sample was divided into three parts and the splits were reacted overnight with 0.5-N, 2-N, or 6-N HCl. The residues were rinsed with distilled H_2O, centrifuged three times, freeze-dried, and again homogenized. Approximately 100 mg of decalcified sediment sample was loaded with Cu-Cu_xO_x reagent, sealed in 6-mm quartz tubes at high vacuum, and combusted at 910°C for 3 hr. TOC concentrations were calculated from CO_2 yields determined using a Hg manometer.

All samples except one used for N concentration and isotopic composition analyses were Leg 205 sediments frozen on board ship. For the N analyses, each sample was divided into three parts. One split was reacted with 6-N HCl overnight, rinsed with distilled H_2O, and centrifuged three times. A second split was only rinsed with distilled H_2O and centrifuged three times. The third split did not receive any pretreatment. About 500–1000 mg of freeze-dried, homogenized sample rinsed with 6-N HCl or distilled H_2O rinsing and mixed with Cu-Cu_xO_x reagent was put into 9-mm quartz tubes, sealed at high-vacuum, and combusted at 910°C for 3 hr (see description of heating routines by Bebout and Fogel, 1992; Sadofsky and Bebout, 2000; Bebout and Sadofsky, 2004). Nitrogen concentrations were determined by measuring the m/z 28 signal for calibrated inlet volumes in the mass spectrometer.

Results and Discussion

Response of Total Organic Carbon to Varying HCl Concentration in Acid Treatments

Concentrations and isotopic ratios of TOC of samples treated with 0.5- to 6-N HCl acid and rinsed three times with H_2O are listed in Table AT1. For all seven of the samples we tested, the three treatments yielded reasonably similar values in both TOC concentrations and $\delta^{13}C$ values, indicating little or no effect of the acid treatments on the integrity of the organic C reservoir.

AT1. HCl concentrations, p. 37.

Effects of H_2O and HCl Treatments on Sediment Nitrogen Concentrations and δ^{15}N

Nitrogen concentrations and δ^{15}N values of untreated sediment, H_2O-rinsed sediment, and sediment treated with 6-N HCl and rinsed with H_2O three times are listed in Table **AT2.** Relative to the untreated splits, the sample splits rinsed with H_2O showed slight decreases in N concentrations but significant increases in δ^{15}N values. Sample splits treated with 6-N HCl then rinsed three times with H_2O showed significant decreases in N concentrations but smaller increases in δ^{15}N values (Fig. **AF1**).

AT2. Pretreatments, p. 38.

AF1. Sample treatment comparison, p. 36.

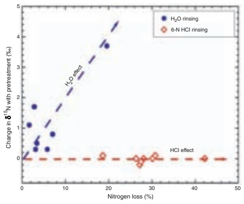

The decrease of N concentrations related to these treatments indicates that certain N species were removed by the H_2O or HCl. In general, distilled H_2O is expected to leach only the more soluble ions/cations, such as ammonium (NH$_4^+$) and nitrate (NO$_3^-$), and maybe some surface-absorbed material. Regarding the two soluble N species, the heavy isotope ^{15}N is preferentially incorporated into nitrate, whereas the light isotope ^{14}N is preferentially incorporated into ammonium (i.e., ammonium has lower δ^{15}N and nitrate has higher δ^{15}N values). The removal of a ^{14}N-enriched N component with distilled H_2O can explain the increase in δ^{15}N of the sediment N. Removal of the ^{15}N-enriched portion would be expected to produce an increase in the sediment δ^{15}N values. In sediments from Legs 170 and 205, interstitial fluid contains hundreds to tens of thousands of parts per million NH$_4^+$ (Kimura, Silver, Blum, et al., 1997), but nitrate data are not yet available. If nitrate is not abundant, the dominant H_2O-mobile N component in these sediments is ammonium, which is consistent with the observation of increase in δ^{15}N values with decrease of N concentrations after H_2O rinsing.

The decrease in the N concentrations of the sediments after 6-N HCl treatment and rinsing with H_2O indicates more dramatic removal than in the treatments with only H_2O. Since there is little or no difference between the δ^{15}N values of the untreated samples and the 6-N HCl–rinsed samples, the N species removed by this treatment, but not the δ^{15}N-only treatments, presumably had heavier N isotopic ratios resulting in a removal of N with averaged δ^{15}N near that of the untreated sediment. Proteins and amino acids, which are characterized by more positive C and N isotopic compositions, could be candidates for these loosely bound but easily acid-decomposed N species. Decrease in δ^{13}C values or TOC concentrations, however, were not observed in our 0.5-N to 6-N HCl treatments (Table **AT1**), implying preferential removal of components with high N/C during the acid treatments. The decoupling of C and N isotopes during sediment decalcification was also documented by Krishnamurthy et al. (1999), and the mechanism remains unclear.

Comparison of Carbon-Nitrogen Data for Air-Dried/Stored, Refrigerated, and Frozen Samples

Based on the comparisons above, we used 1-N HCl rinsing pretreatment for TOC analyses and unpretreated samples for the TN analyses for all other sediments from Site 1040 and all but the three samples from Hole 1255A that were pretreated using distilled H_2O or by 6-N HCl treatment followed by rinsing with H_2O. The results are shown in Figures **F2** and **F3.** On these figures, it is evident that the air-dried/stored samples from the Site 1040 sediments yielded C and N concentrations and isotopic compositions quite similar to those of the refrigerated or freeze-dried sediments from Site 1040 from similar depths. The samples are generally collected from several centimeters away (Table AT2), or at the least, falling within the range of natural scatter in the core. Furthermore, the data for Hole 1254A overlap well with those for Site 1040 in both TOC and TN concentrations and isotopic compositions but with a small number of outliers. The three samples from Hole 1255A show more variation in C and N concentrations and isotopic compositions, Variations for N are partly a result of the different pretreatments for the N determinations, but are possibly also related to the natural sediment heterogeneity. The consistency in C and N concentrations and isotopic compositions between these differentially preserved samples indicates that room-temperature-air dried sediments should be suitable for organic C-N geochemical study. This conclusion might also be extended to the low-temperature heated samples, which are dried in a drying oven at 40°–60°C (Minoura et al., 1997; Tolun et al., 2002; Sadofsky and Bebout, 2004).

Figure F1. **A.** Central America convergent margin, locations of Legs 170 and 205, and isochrons derived from seafloor magnetic anomalies. Numbers indicate crustal age in millions of years. Tectonic boundaries, convergence direction and rate (arrow), and arc volcanoes (triangles) are also shown. FS = Fisher Seamount, QSC = Quesada Sharp Contortion. (Continued on next three pages.)

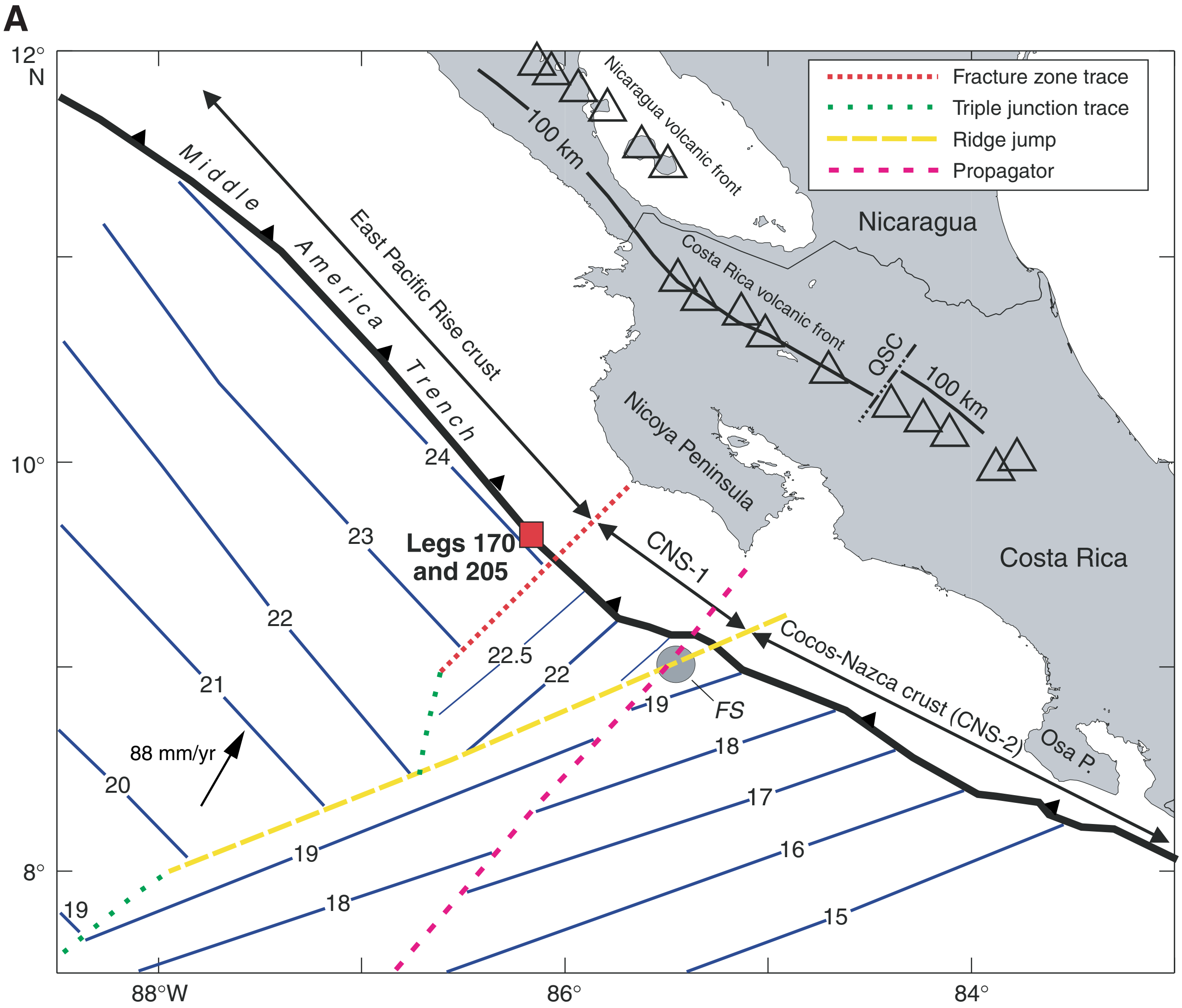

Figure F1 (continued). B. Bathymetric map of Legs 170 and 205 with detailed locations of each site.

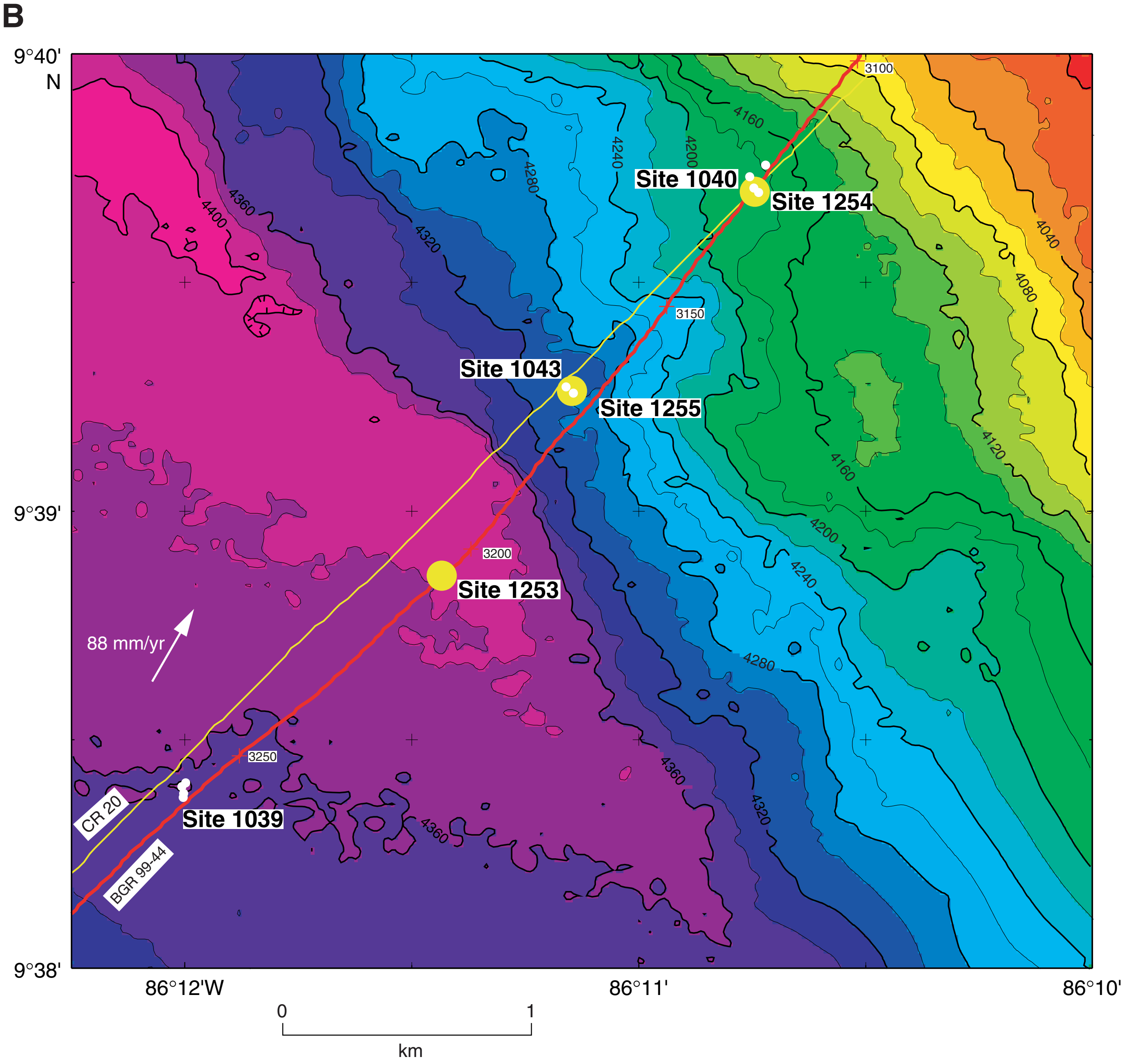

Figure F1 (continued). **C.** Migrated multichannel seismic Cross-section BGR-99-44 showing Sites 1039, 1040, and 1043 (thin lines) and Sites 1253, 1254, and 1255 (thick lines). CMP = common midpoint.

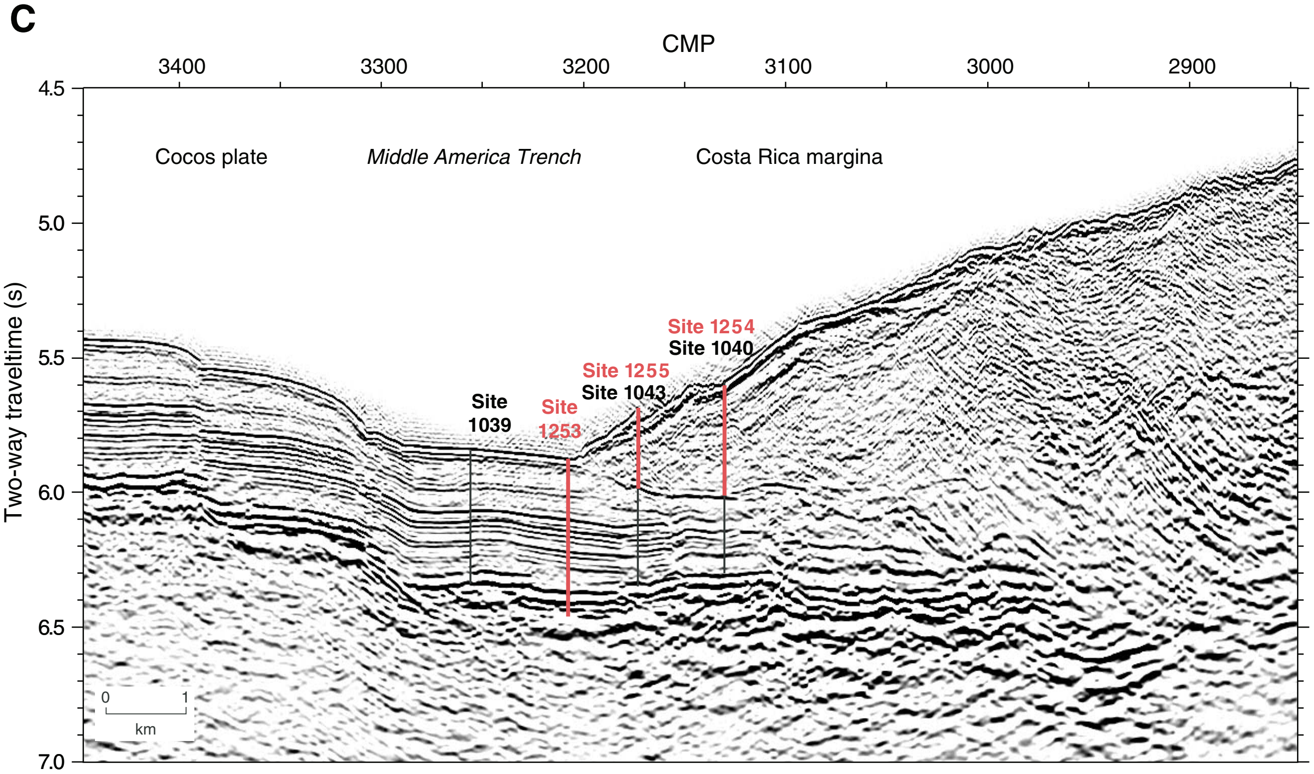

Figure F1 (continued). D. Lithology of sediments recovered from Sites 1040 and 1043 in the wedge. Lithology at Sites 495 and 1039 in the incoming plate is also shown for comparison.

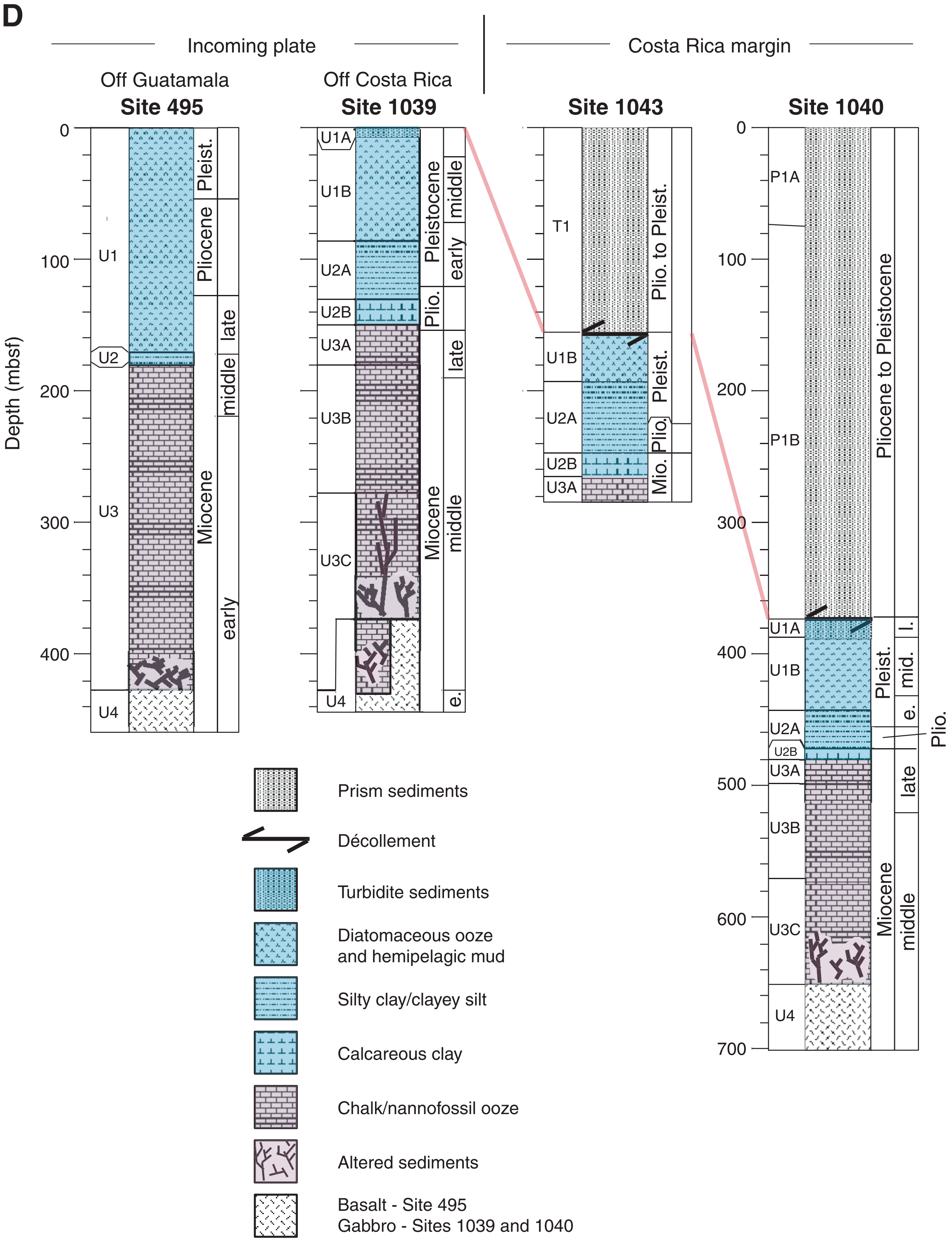

Figure F2. Nitrogen concentrations and isotopic compositions at Sites 1040, 1254 and 1255. Patterned areas represent fault zones and the décollement. Note the covariation and significant downhole increase in N concentrations and isotopic compositions of sediments and ammonium compositions of interstitial fluid. Also noteworthy is the hint of change in N concentrations and isotopic compositions of sediments along contacts between fault zones and wall sediments. **A.** Downhole variation of N concentrations of sediments. The data from Site 1040 are consistent with those for Sites 1254 and 1255, as well as those presented for Site 1040 by Kimura, Silver, Blum, et al., 1997. **B.** Downhole $\delta^{15}N$ variation of sediments. Data from Sites 1040, 1254, and 1255 are consistent with each other. **C.** Downhole variation of ammonium concentrations of interstitial fluid. Data from Kimura, Silver, Blum, et al., 1997.

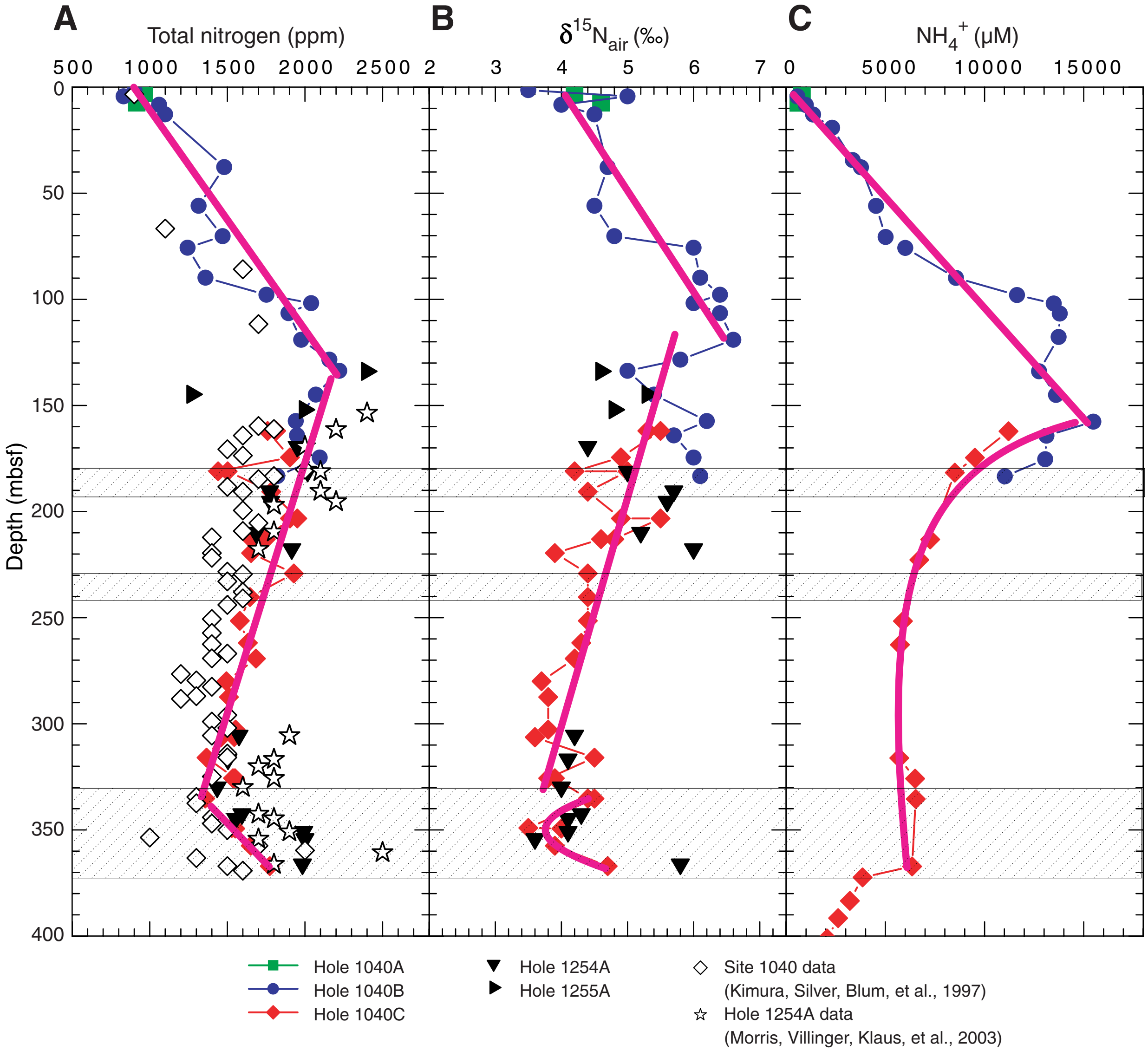

Figure F3. Total organic carbon (TOC) concentration and isotopic data of sediments from Sites 1040, 1254 and 1255. Patterned areas represent fault zones and the décollement. **A.** Downhole concentration variation of TOC. The values are slightly higher than those of Kimura, Silver, Blum, et al. (1997). **B.** Downhole variation of $\delta^{13}C$. VPDB = Vienna Peedee belemnite. **C.** TOC/total nitrogen (TN) variation with depth. Sediments from 1040, 1254, and 1255 show congruent values in TOC concentrations, $\delta^{13}C$ values, and TOC/TN ratios. Note the downhole decrease in TOC/TN ratios, largely related to downhole increase in TN concentration, in the uppermost ~100 m.

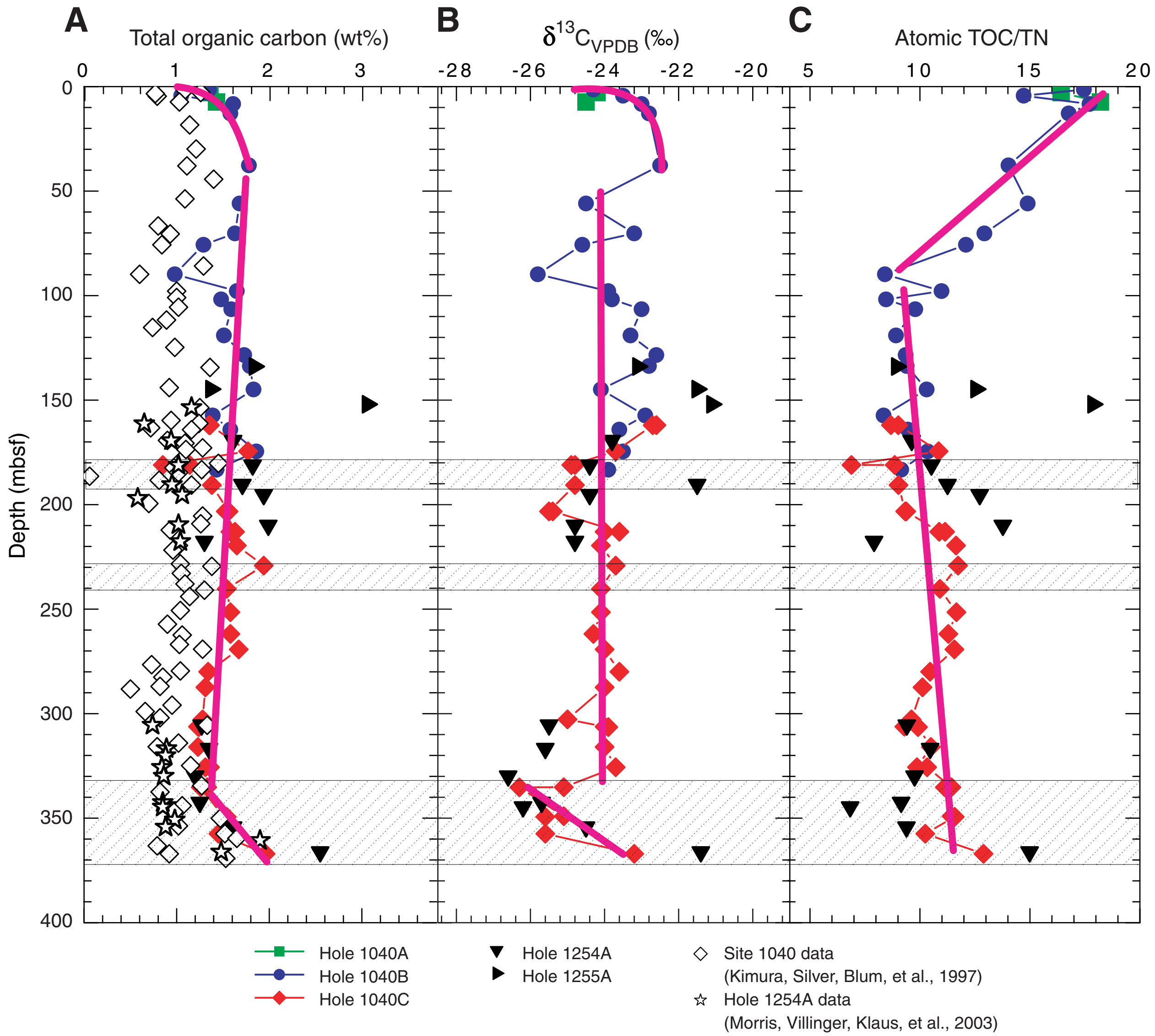

Figure F4. Carbonate concentrations and its C- and O-isotope compositions of sediments from Site 1040. Patterned areas represent fault zones and the décollement. **A.** Downhole variation of carbonate concentration. Concentrations are all <4 wt% and lower than those of Kimura, Silver, Blum, et al. (1997). **B.** Downhole $\delta^{13}C$ variations. Note that one sediment shows a value of –26.1‰ and several samples have $\delta^{13}C$ lower than –5‰. VPDB = Vienna Peedee belemnite. **C.** Downhole $\delta^{18}O$ variations. There is no relationship between structural position, relative to fault zones and the décollement, and carbonate concentrations and isotopic compositions. VSMOW = Vienna standard mean ocean water.

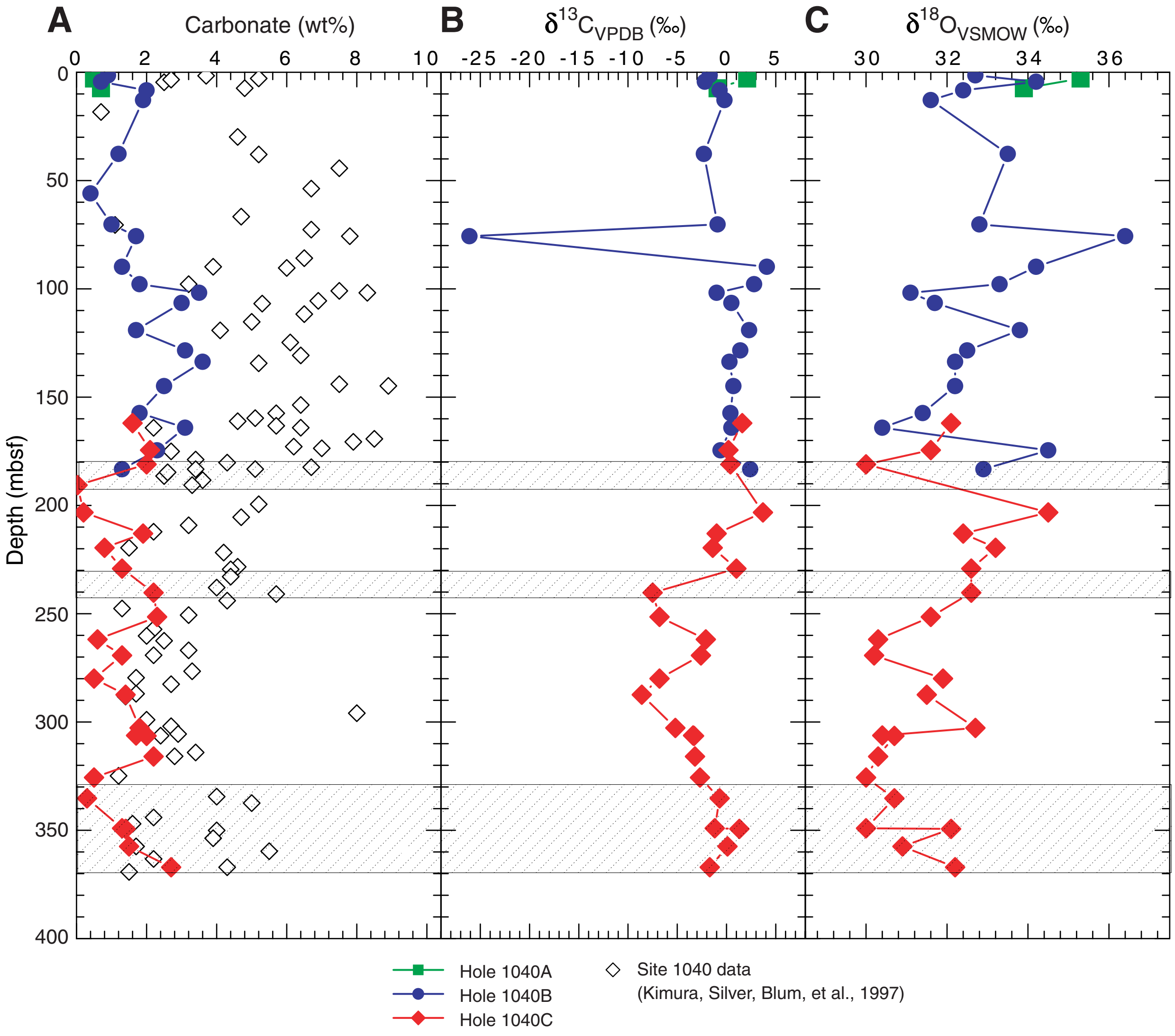

Figure F5. Plot of concentration vs. isotope composition of total organic carbon (TOC) and total nitrogen (TN) of sediments from Site 1040. The data are divided factitiously into two groups: uppermost 8 mbsf and below 8 mbsf. Data for samples below 8 mbsf show a crude negative relationship between concentrations and isotope compositions. Data for samples in the uppermost 8 mbsf show a weak positive linear correlation of concentrations and isotope compositions. VPDB = Vienna Peedee belemnite.

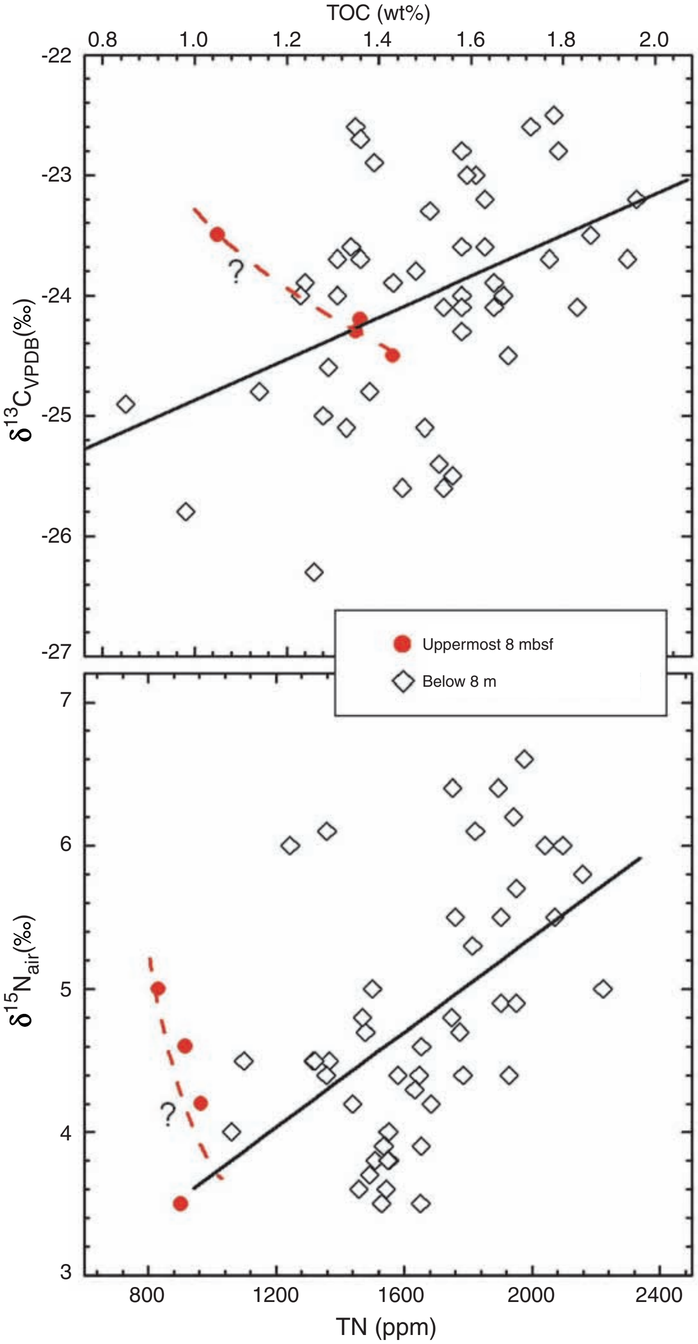

Figure F6. δ^{15}N-δ^{13}C diagram of sediments from Site 1040, including data for Sites 1254 and 1255. The distribution of Site 1040 data shows deflecting trend from the mixing line between terrestrial and marine organic components proposed by Minoura et al. (1997). Both diagenetic alteration similar to that of Site 1149 (Sadofsky and Bebout, 2004) and a ^{13}C-depleted terrestrial source may have contributed to this deflection. VPDB = Vienna Peedee belemnite.

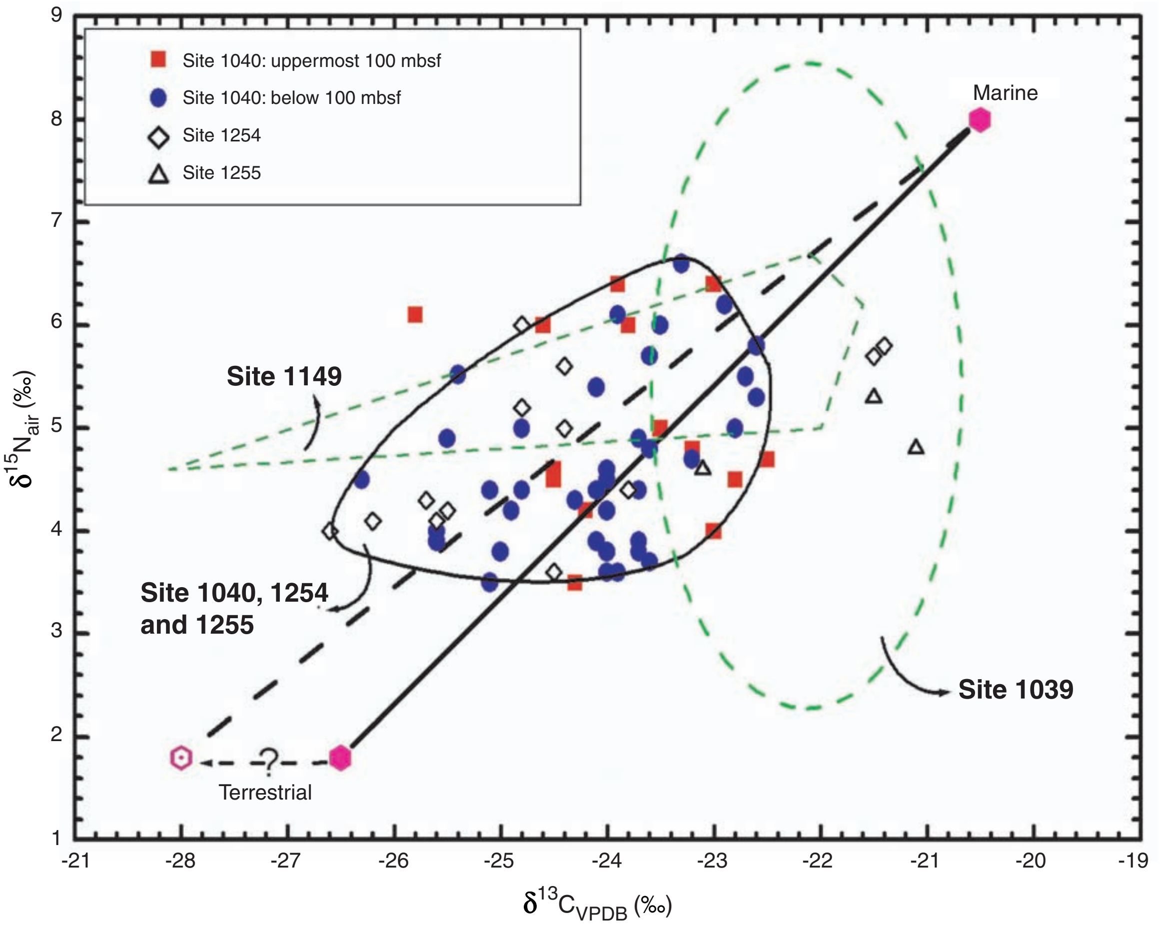

Figure F7. Depth-converted seismic Section CR-20 crossing Sites 1039, 1040, 1041, and 1043 (from Silver, 2000). Note the positions of the deformed wedge, slope apron, and drill sites discussed in the text.

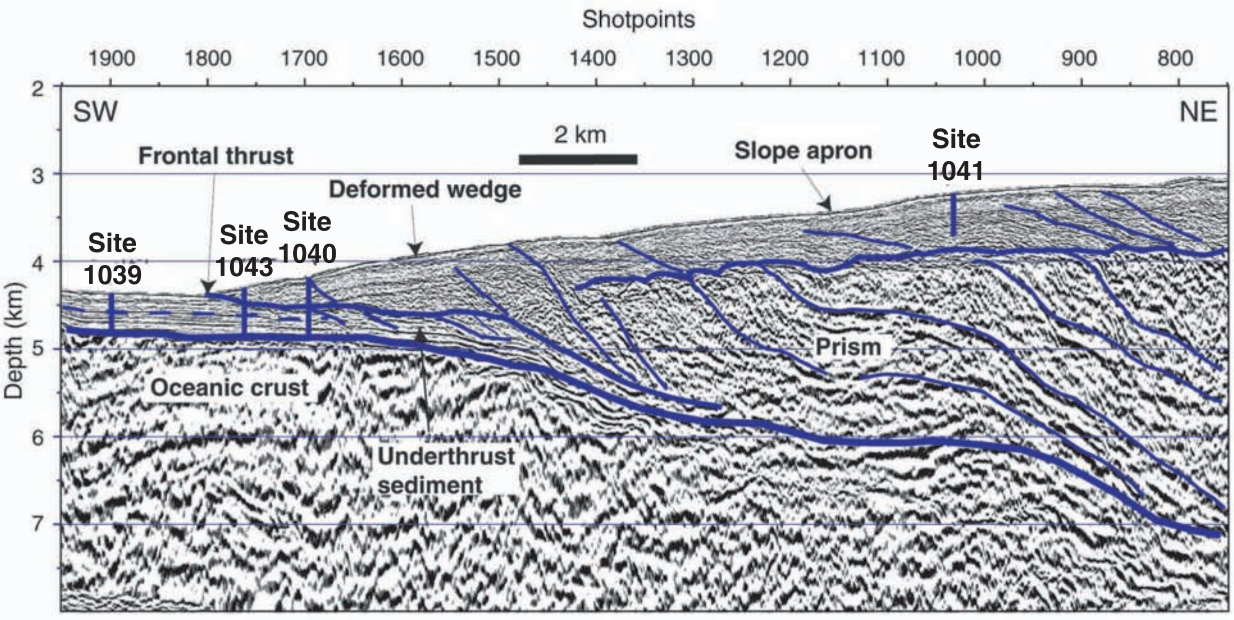

Table T1. Carbon and nitrogen concentrations and isotopic compositions of sediments from Sites 1040, 1254, and 1255. (**See table notes.** Continued on next page.)

			Nitrogen		Organic carbon			Carbonate		
Core, section, interval (cm)	Depth (mbsf)	Description	TN (ppm)	$\delta^{15}N_{air}$ (‰)	TOC (wt%)	$\delta^{13}C_{VPDB}$ (‰)	Atomic TOC/TN	Total (wt%)	$\delta^{13}C_{VPDB}$ (‰)	$\delta^{18}O_{VSMOW}$ (‰)
170-1040A-										
1H-2, 140–150	2.9		966	4.2	1.36	–24.2	16.4	0.5	2.1	35.3
1H-5, 140–150	7.4		916	4.6	1.43	–24.5	18.2	0.7	–0.9	33.9
170-1040B-										
1H-1, 140–150	1.4	Silty clay to clayey silt with debris flows and silty sands	902	3.5	1.35	–24.3	17.5	0.9	–1.7	32.7
1H-3, 135–150	4.35		832	5.0	1.05	–23.5	14.7	0.7	–2.2	34.2
2H-2, 125–150	8.35		1060	4.0	1.61	–23	17.7	2.0	–0.7	32.4
2H-5, 125–150	12.85		1099	4.5	1.58	–22.8	16.8	1.9	–0.2	31.6
6X-1, 130–150	37.7		1480	4.7	1.78	–22.5	14	1.2	–2.3	33.5
8X-1, 74–84	55.94		1315	4.5	1.68	–24.5	14.9	0.4		
9X-4, 124–144	70.26		1470	4.8	1.63	–23.2	12.9	1.0	–0.9	32.8
10X-1, 130–150	75.7	Silty clay (stone)	1244	6.0	1.29	–24.6	12.1	1.7	–26.1	36.4
11X-4, 130–150	89.8		1359	6.1	0.98	–25.8	8.4	1.3	4.1	34.2
12X-3, 125–150	97.85		1752	6.4	1.65	–23.9	11	1.8	2.8	33.3
13X-2, 120–150	101.8		2040	6.0	1.48	–23.8	8.5	3.5	–1	31.1
14X-2, 120–150	106.5		1894	6.4	1.59	–23	9.8	3.0	0.5	31.7
15X-4, 120–150	119.05		1976	6.6	1.51	–23.3	8.9	1.7	2.3	33.8
16X-5, 125–150	128.45		2157	5.8	1.73	–22.6	9.4	3.1	1.4	32.5
17X-1, 120–150	133.7		2221	5.0	1.79	–22.8	9.4	3.6	0.3	32.2
18X-2, 120–150	144.90		2070	5.5	1.83	–24.1	10.3	2.5	0.7	32.2
19X-4, 120–150	157.35		1941	6.2	1.39	–22.9	8.4	1.8	0.4	31.4
20X-2, 120–150	164.1		1949	5.7	1.58	–23.6	9.5	3.1	0.5	30.4
21X-3, 120–150	174.57		2095	6.0	1.86	–23.5	10.4	2.3	–0.6	34.5
22X-2, 120–150	183.3		1822	6.1	1.43	–23.9	9.2	1.3	2.4	32.9
170-1040C-										
1R-2, 117–119[*]	161.97		1814	5.3	1.35[†]	–22.6[†]	8.7			
1R-2, 120–150	162.00		1759	5.5	1.36	–22.7	9.0	1.6	1.6	32.1
2R-4, 115–150	174.45		1903	4.9	1.77	–23.7	10.8	2.1	0.2	31.6
3R-2, 111–113[*]	181.01		1440	4.2	0.85	–24.9	6.9			
3R-2, 115–150	181.05		1502	5.0	1.14	–24.8	8.9	2.0	0.4	30.0
4R-2, 120–150	190.65		1783	4.4	1.38	–24.8	9.0	0.03		
5R-4, 112–114[*]	203.22		1950	4.9	1.56[†]	–25.5[†]	9.3			
5R-4, 115–150	203.25		1903[‡]	5.52[‡]	1.53	–25.4	9.3	0.2	3.7	34.5
6R-4, 117–119[*]	212.97		1748	4.8	1.63	–23.6	10.9			
6R-4, 120–150	213.00		1654	4.6	1.58	–24	11.1	1.9	–1.0	32.4
7R-2, 117–119[*]	219.57		1653	3.9	1.65	–24.1	11.6	0.8	–1.4	33.2
8R-2, 115–150	229.15		1928	4.4	1.94	–23.7	11.7	1.3	1.0	32.6
9R-3, 115–150	240.31		1646	4.4	1.54	–24.1	10.9	2.2	–7.5	32.6
10R-4, 115–150	251.45		1580	4.4	1.58	–24.1	11.7	2.3	–6.8	31.6
11R-5, 115–150	261.86		1632	4.3	1.58	–24.3	11.3	0.6	–2.1	30.3
12R-3, 115–150	269.25		1684	4.2	1.67	–24	11.6	1.3	–2.6	30.2
13R-4, 75–100	279.95		1494	3.7	1.34	–23.6	10.5	0.5	–6.8	31.9
14R-3, 0–35	287.40		1510	3.8	1.31	–24	10.1	1.4	–8.6	31.5
15R-6, 115–150	302.75		1553	3.8	1.28	–25	9.6	1.8	–5.2	32.7
16R-2, 102–106[*]	306.22		1544	3.6	1.23	–24	9.3	1.7	–3.4	30.4
16R-2, 120–150	306.40		1459	3.6	1.24	–23.9	9.9	2.0	–3.3	30.7
17R-2, 115–150	315.95		1366	4.5	1.23	–24	10.5	2.2	–3.2	30.3
18R-2, 112–115[*]	325.62		1549	3.8	1.31[†]	–23.7[†]	9.9			
18R-2, 115–150	325.65		1536	3.9	1.36	–23.7	10.3	0.5	–2.7	30.0
19R-2, 112–115[*]	335.22		1357	4.4	1.33[†]	–25.1[†]	11.4			
19R-2, 115–150	335.25		1320	4.5	1.26	–26.3	11.1	0.3	–0.7	30.7
20R-5, 88–94[*]	349.08		1529	3.5	1.5	–25.1	11.4	1.3	–1.2	30.0
20R-5, 115–150	349.35		1551	4.0	1.54	–25.6	11.6	1.4	1.3	32.1
21R-4, 115–150	357.45		1651	3.5	1.45	–25.6	10.2	1.5	0.1	30.9
22R-4, 115–150	367.05		1773	4.7	1.96	–23.2	12.9	2.7	–1.7	32.2

Table T1 (continued).

			Nitrogen		Organic carbon			Carbonate		
Core, section, interval (cm)	Depth (mbsf)	Description	TN (ppm)	$\delta^{15}N_{air}$ (‰)	TOC (wt%)	$\delta^{13}C_{VPDB}$ (‰)	Atomic TOC/TN	Total (wt%)	$\delta^{13}C_{VPDB}$ (‰)	$\delta^{18}O_{VSMOW}$ (‰)
205-1254A-										
3R-3, 125–165	169.35	Clay with intervals of silt to very fine sand	1950	4.4	1.61	–23.8	9.6			
4R-5, 45–90	181.11		2017	5.0	1.82	–24.4	10.5			
5R-5, 50–90	190.40		1772[‡]	5.7[‡]	1.71	–21.5	11.3			
6R-1, 121–162	195.31		1779[‡]	5.6[‡]	1.94[†]	–24.4[†]	12.7			
7R-5, 34–74	209.95		1685[‡]	5.2[‡]	1.99	–24.8	13.8			
8R-4, 0–45	217.65		1915[‡]	6.0[‡]	1.3	–24.8	7.9			
9R-5, 0–40	305.50		1575	4.2	1.27	–25.5	9.4			
10R-6, 0–40	316.73		1504[‡]	4.1[‡]	1.35	–25.6	10.5			
12R-1, 101–141	329.91		1434[‡]	4.0[‡]	1.20[†]	–26.6[†]	9.8			
13R-3, 100–145	342.50		1594	4.3	1.25[†]	–25.7[†]	9.1			
13R-5, 65–109	344.65		1554[‡]	4.1[‡]	0.91	–26.2	6.8			
14R-3, 0–40	350.81		1992	4.1						
14R-6, 52–97	354.28		2000	3.6	1.61	–24.5	9.4			
16R-3, 49–89	366.19		1984	5.8	2.55	–21.4	15.0			
205-1255A-										
2R-2, 0–43	133.94	Silty clay and breccia	2398[††]	4.6[††]	1.84	–23.1	8.9			
3R-2, 87–127	144.77	Diatom ooze	1273**	5.3**	1.37	–21.5	12.6			
4R-1, 0–38	152.00		1997**	4.8**	3.06	–21.1	17.9			

Notes: Site 1040 samples were kept at room temperature and naturally dried unless otherwise indicated. TN = total nitrogen, TOC = total organic carbon, VPDB = Vienna Peedee belemnite, VSMOW = Vienna standard mean ocean water. * = cold-stored sample for comparison, † = average data listed in Table AT1, p. 37, ‡ = untreated sample data listed in Table AT2, p. 38, ** = sample rinsed with distilled water before analysis, †† = sample rinsed with 6-N HCl before analysis.

Figure AF1. Comparison of N concentrations and isotopic compositions of untreated samples and H_2O- and 6-N HCl-rinsed samples, showing that H_2O tends to remove a small fraction of N with lighter N isotopic species, possibly ammonium cation, and HCl tends to remove a larger fraction of N without an isotopic preference, perhaps a combination of N as free ions/cations, surface absorbed material, and loosely bound organic N. See Table AT2, p. 38, for data.

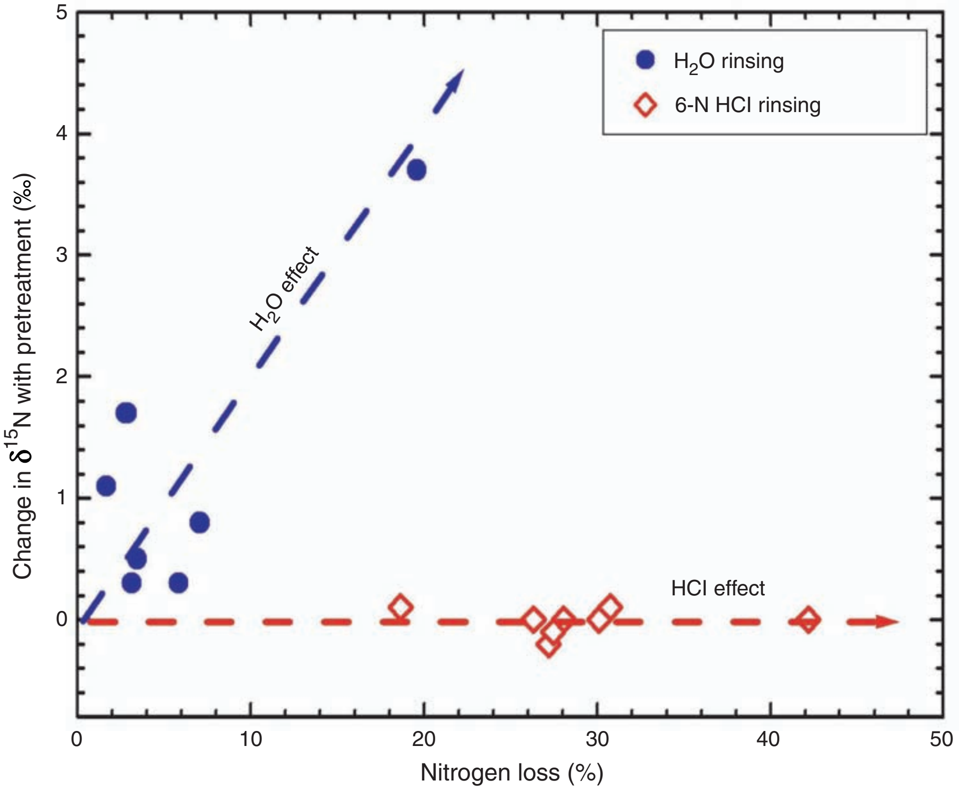

Table AT1. Total organic carbon concentrations and isotope compositions of sediments decalcified with varying HCl concentrations.

Core, section, interval (cm)	HCl concentration (N)	TOC (wt%)	$\delta^{13}C_{VPDB}$ (‰)
170-1040C-			
1R-2, 117–119	0.5	1.34	–22.6
	2	1.35	–22.6
	6	1.36	–22.7
5R-4, 112–114	0.5	1.53	–25.6
	2	1.61	–25.4
	6	1.53	–25.6
18R-2, 112–115	0.5	1.32	–23.7
	2	1.33	–23.7
	6	1.29	–23.7
19R-2, 112–115	0.5	1.31	–25.2
	2	1.35	–25.1
	6	1.32	–25
205-1254A-			
6R-1, 121–162	0.5	2	–24.3
	2	1.89	–24.3
	6	1.92	–24.5
12R-1, 101–141	0.5	1.22	–26.5
	2	1.19	–26.8
	6	1.18	–26.6
13R-3, 100–145	0.5	1.27	–25.6
	2	1.22	–25.7
	6	1.25	–25.9

Notes: All samples used for comparisons were either frozen onboard immediately upon recovery (Leg 205) or stored refrigerated for a prolonged period (Leg 170) at ODP Gulf Coast Core Repository (College Station, Texas). TOC = total organic carbon, VPDB = Vienna Peedee belemnite.

Table AT2. Nitrogen concentrations and isotope compositions of sediments using varying pretreatments.

Core, section, interval (cm)	Pretreatment	N (ppm)	$\delta^{15}N_{air}$ (‰)
170-1040C-			
5R-4, 115–150	None	1903	5.5
	H_2O rinsing	1530	9.2
	6-N HCl rinsing	1100	5.5
205-1254A-			
5R-5, 50–90	None	1772	5.7
	H_2O rinsing	1716	6.0
	6-N HCl rinsing	1227	5.8
6R-1, 121–162	None	1779	5.6
	H_2O rinsing	1675	5.9
	6-N HCl rinsing	1295	5.4
7R-5, 34–74	None	1685	5.2
	H_2O rinsing	1637	6.9
	6-N HCl rinsing	1212	5.2
8R-4, 0–45	None	1915	6.0
	H_2O rinsing	1849	6.5
	6-N HCl rinsing	1558	6.1
10R-6, 0–40	None	1504	4.1
	H_2O rinsing	1479	5.2
	6-N HCl rinsing	1108	4.1
12R-1, 101–141	None	1434	4.0
	H_2O rinsing	1394	5.7
	6-N HCl rinsing	1002	4.0
13R-5, 65–109	None	1554	4.1
	H_2O rinsing	1444	4.9
	6-N HCl rinsing	1127	4.0

Notes: Leg 205 samples were frozen onboard and sent frozen to Lehigh University. Leg 170 sample was air-dried and stored as a dried powder.